Sulfonated Polymer Metal Nanocomposite Membranes with Bacterial Disinfection Activity in Water

by

Nataira Marie Pagán-Pagán

A thesis submitted in partial fulfillment of the requirements for the degree of

MASTER of SCIENCE

in

CHEMICAL ENGINEERING

UNIVERSITY of PUERTO RICO

MAYAGÜEZ CAMPUS

2018

Approved by:

_____	_____
David Suleiman Rosado, PhD Graduate Committee President	Date
_____	_____
Pedro J. Tarafa Vélez, PhD Graduate Committee Member	Date
_____	_____
Moses N. Bogere, PhD Graduate Committee Member	Date
_____	_____
Rafael R. Montalvo Rodríguez, PhD Graduate Committee Member	Date
_____	_____
José E. Cortés Figueroa, PhD Graduate Studies Representative	Date
_____	_____
Aldo Acevedo Rullán, PhD Chairperson of the Department	Date

DEDICATION

This thesis is dedicated

to my beloved parents, Joaquín and María,

who have always been my inspiration,

to my brothers, Joaquín Josué and Joaquín Joshua,

and my niece Tairalee,

for always being there for me,

and to the love of my life, Oscar,

and my dearest daughter, Catalina,

for who I dare to dream.

ACKNOWLEDGEMENTS

I would like to express my special gratitude and thanks to my research advisor, Dr. David Suleiman, who believed in me and my intellectual curiosity, for his guidance and academic support. I would also like to thank distinguished members of my dissertation committee, Dr. Pedro Tarafa, Dr. Moses Bogere and Dr. Rafael Montalvo, for their time and valuable discussions.

I would like to acknowledge Dr. Suleiman laboratory members and my colleagues, Dr. Maritza Pérez, Dr. Edward Guerrero, Eduardo Ruiz, Karen Barrios, Liliana Villanueva, and Claudia Feliciano for helping me accomplish the experiments and for their support. I would also like to acknowledge Amarillys Avilés for her collaboration with the bactericide evaluation experiments.

Finally, I would like to acknowledge the Puerto Rico Science, Technology and Research Trust for providing the financial support.

ABSTRACT

This study describes the synthesis and characterization of sulfonated poly(styrene-isobutylene-styrene) (SIBS) polymer nanocomposite membranes, which show antibacterial properties useful for the inactivation of *Enterococci* and *Escherichia coli* (*E. coli*) pathogenic bacteria present in surface waters, particularly when cupric (Cu^{2+}) and ferric (Fe^{3+}) counter-ions were cross-linked to the membrane. The antibacterial evaluation of copper-exchanged and iron-exchanged sulfonated SIBS was carried out by assaying the presence of *Enterococci* and *E. coli* bacteria after the membranes were brought into contact with bacteria suspensions. Overall, the cell viability results obtained suggested that *Enterococci* was more susceptible to inactivation than *E. coli* and that copper-exchanged sulfonated SIBS successfully inactivated most of both pathogenic bacteria. It was found that copper-exchanged sulfonated SIBS was more selective to *E. coli* and iron-exchanged sulfonated SIBS was more selective to *Enterococci* bacteria although the extent of inactivation varied depending on the water source, treatment time, the water sample volume and initial concentration of the bacteria suspensions. Moreover, it was observed that the inactivation of *E. coli* was strongly influenced by the degree of sulfonation, since it was found to be dependent on the quantity of the Cu^{2+} exchanged in the copper-exchanged sulfonated SIBS membrane. The physico-chemical properties of copper-exchanged and iron-exchanged sulfonated SIBS were influenced by the exposure to bacteria suspensions nevertheless, the antibacterial properties of the membranes were not compromised since, with reusable membranes, nearly 0% cell viability was obtained.

RESUMEN

Este estudio describe la síntesis y caracterización de membranas poli(estireno-isobutileno-estireno) (SIBS) sulfonado, las cuales presentan propiedades antibacterianas útiles para la inactivación de bacterias patógenas *Enterococci* y *Escherichia coli* (*E. coli*), las cuales están presentes en aguas superficiales, particularmente cuando contraiones cúpricos (Cu^{+2}) y férricos (Fe^{3+}) se entrelazan en la membrana. La evaluación antibacteriana de SIBS sulfonado intercambiado con cobre e intercambiado con hierro se llevó a cabo mediante el ensayo de la presencia de bacterias *Enterococci* y *E. coli*, después de que las membranas se pusieran en contacto con suspensiones de bacterias. En general, los resultados obtenidos de viabilidad celular sugirieron que las bacterias *Enterococci* eran más susceptibles a la inactivación que las bacterias *E. coli*, y que membranas de SIBS sulfonado intercambiado con cobre inactivaban la mayoría de las bacterias patógenas. Se encontró que el SIBS sulfonado intercambiado con cobre era más selectivo a bacterias *E. coli* y el SIBS sulfonado intercambiado con hierro era más selectivo a bacterias *Enterococci*, aunque el grado de inactivación variaba según la fuente de agua, el tiempo de tratamiento, el volumen de agua de la muestra analizada y la concentración inicial de las suspensiones de bacteria. Además, se observó que la inactivación de *E. coli* estaba fuertemente influenciada por el grado de sulfonación, ya que se encontró que la inactivación dependía de la cantidad de Cu^{2+} intercambiado en la membrana SIBS sulfonada. Las propiedades físico-químicas de SIBS sulfonado intercambiado con cobre e intercambiado con hierro se vieron influenciadas por la exposición a suspensiones de bacterias, sin embargo, las propiedades antibacterianas de las membranas no se vieron comprometidas ya que, con membranas reutilizables, se obtuvo casi 0% de viabilidad celular.

TABLE of CONTENTS

LIST of FIGURES

LIST of TABLES

1 Introduction

1.1. Introduction

Access to safe drinking water is needed to sustain life, therefore to ensure a good quality of drinking water sources represents tangible benefits for the health and well-being of humans.[1,2] Proactive approaches towards sustainable access to safe drinking water have provided the lead for the development of increasingly prevalent water system supplies in communities where there exists lack of safe drinking water sources.[2,3] Because of the meaningful understanding of the quality and safety requirements of drinking water, 2.6 billion people around the world find the most appropriate and secure sources of drinking water through piped water on premises.[1,3,4] Unfortunately, these improved drinking water sources are not the only ones available since there exist unimproved drinking water sources, whose direct consumption must be avoided because it may exhibit significant risks to the human health.[4,5] However, in 2015, 663 million people around the world used water from unprotected wells, surface waters, among other sources representing no evidence of treatment or which are not meeting the water quality criteria required to qualify as safe drinking water.[3]

The World Health Organization (WHO) estimates that the majority of those who do not have access to safe drinking water is among people living in rural areas and that 93% of these use surface waters as their main source of drinking water.[3] The vulnerability of surface waters to fecal contamination is critical. Due to geographical location, the lack of sanitation, industrial or agricultural activities, and residual water discharges, surface waters may be increasingly contaminated as pathogens may naturally infiltrate the water sources.[1,2] Regardless of the source of contamination, such drinking water sources may represent a threat to the health and well-being of the 159 million people in the world who still use fecally contaminated surface waters to satisfy their needs.[2,3]

Despite the progress in the development of safe drinking water supplies around the world, in 2012, it was reported that 1.8 billion people could not assure safe drinking water since the only means available for the access of drinking water were fecally contaminated.[3] The most common health risk associated with microbial hazards is the potential to cause waterborne diseases such as diarrhea, and in very severe cases may cause death.[2,8] Hence, the microbial contamination control is not to be neglected and must always be of vital importance to assure safe drinking water.[1]

Although pathogenic bacteria constitute a minor portion of all bacterial species, these are the most abundant pathogenic microorganisms in surface waters.[9] While most pathogenic bacteria of fecal origin are unable to survive indefinitely in the environment, *Escherichia coli* (*E. coli*) have been reported to survive indefinitely in surface waters thus serving the purpose of an indicator of fecal contamination.[1,10,11] *E. coli* provides conclusive evidence of fecal contamination in surface waters yet its absence will not necessarily reveal the possible existence of other pathogenic microorganisms.[1] In such cases, the use of a more resistant fecal indicator such as intestinal *Enterococci* may be more appropriate.[1] According to the Environmental Protection Agency (EPA)

of the United States, surface waters must meet the *Bacteriological Ambient Water Quality Criteria* established in 1986, which states that both *E. coli* and *Enterococci* pathogenic bacteria should not exceed the 126 colony forming units (CFU) per 100 mL (CFU/100 mL) and 33 CFU/100 mL, respectively.[3,6,7]

While pathogenicity is an important characteristic of both *E. coli* and *Enterococci*, understanding fundamental characteristics of their structure and its constituents helps to elucidate the effect these bacteria have in drinking water and their susceptibility to inactivation, which leads to the death of the pathogenic bacteria, as a result of a possible damage in its outer membrane or cell wall, respectively.[9,12,13] Based on the presence of major chemical components in their particular surface layers, *E. coli* could be classified as Gram-negative and *Enterococci* as Gram-positive bacteria.[9] While Gram-negative bacteria shows a complex cell envelope with an outer membrane, its surface exhibits a negative charge due to the presence of negatively charged phospholipids.[9,14,15] On the other hand, the principal surface layer of Gram-positive bacteria is a cell wall with a rigid structure containing highly negatively charged components known as teichoic acids and proteins.[9,16] Among these pathogenic bacteria, the diversity increases the complexity of the interactions with their surroundings, as variabilities may have a large impact and may also difficult the efficiency of their inactivation.

Fulfilling microbial safety of drinking water can be achieved by deliberately using polymers with antimicrobial properties.[14,16–19] Although it has been difficult to predict the nature of the inactivation effects of pathogenic bacteria, the antimicrobial potential of polymers has been efficiently harnessed.[13,16,17,20] For instance, antimicrobial polymers have been proven to avoid resistance of pathogenic bacteria to certain antimicrobial agents such as antibiotics.[14,21] Furthermore, the antimicrobial properties of polymers could be enhanced by the incorporation of

metal nanoparticles, such as copper and iron, giving rise to polymer-metal nanocomposites membranes (PNMs).[16,17,22–24] In recent years, the use of PNMs with antimicrobial properties has shown potential for inactivating pathogenic bacteria by releasing antimicrobial agents.[16,17,19] However, among other advanced antimicrobial materials, polymers are preferred in antimicrobial applications due to the ease in successfully inactivate pathogenic bacteria upon contact and minimizing the risks of post-contamination of the drinking water treated.[17,20]

It has been reported that polystyrene inhibits the growth of *E. coli* and when sulfonic acid groups are incorporated, the nanocomposite inactivates 99.99% of the pathogenic bacteria.[16,25] Hence, the concerns for developing safe drinking water through the inactivation of pathogenic bacteria can be addressed through the use of styrenic thermoplastic elastomers (TPE).[16,26] Poly(styrene-isobutylene-styrene) (SIBS) is a styrenic TPE that has been used in biomedical applications because of its versatile physico-chemical properties.[26–30] SIBS is often functionalized with the incorporation of sulfonic acid groups whose ion exchange sites could be substituted with cupric (Cu^{2+}) and ferric (Fe^{3+}) counter-ions to enhance its physico-chemical and antimicrobial properties.[24,26–28]

This work provides an overview of the development of advanced antimicrobial polymers capable of inactivating pathogenic bacteria as an alternative to achieve safe drinking water. The focus is on the relevant SIBS polymer material for *E. coli* and *Enterococci* bacteria inactivation applications.

1.2. Aims of the proposed work

The goals of this research work include:

- Synthesis of sulfonated SIBS polymer metal nanocomposite membranes

- Comprehensive materials characterization using elemental analysis (EA), ion exchange capacity (IEC), Fourier transform infrared spectroscopy (FT-IR), thermogravimetric analysis (TGA), small-angle X-ray scattering (SAXS), atomic force microscopy (AFM), water uptake (WU), and instrumental neutron activation analysis (INAA)
- Evaluate the feasibility of the antibacterial properties of sulfonated SIBS polymer metal nanocomposite membranes against *E. faecalis* and *E. coli* pathogenic bacteria in terms of the of degree of sulfonation and counter-ion exchanged
- Study of the effect of exposure time, volume and concentration process variables
- Examine the reusability of sulfonated SIBS polymer metal nanocomposite membranes

2 Methodology

2.1. Materials

The polymer used was SIBS (Kaneka®), composed of 30 wt% polystyrene and 70 wt% isobutylene. Methylene chloride (Fisher Scientific, 99.8%), sulfuric acid (Sigma Aldrich, 95-98%), hexyl alcohol (Aldrich Chemical, 98%), and methanol (Fisher Scientific, 99.9%) were used as solvents. For counter-ion substitution, copper chloride ($CuCl_2$) (Sigma-Aldrich, anhydrous powder, 99.99%) and ferric chloride ($FeCl_3$) (Sigma-Aldrich, anhydrous powder, 99.99%) were used. Commercial phosphate buffer (Hardy Diagnostics, Butterfield Buffer D599) was used as received. For the phosphate buffered dilution water prepared in the laboratory, monopotassium phosphate monobasic anhydrous (KH_2PO_4, CAS No. 7778-77-0) and magnesium chloride ($MgCl_2$, CAS No. 7786-30-3) were used. Deionized (DI) water was used to prepare solutions, wash the polymer and membranes.

2.2. Materials preparation

2.2.1. *Polymer sulfonation*

Sulfonation of SIBS was performed according to a procedure reported by Avilés-Barreto.[28] Approximately 30 g of SIBS was weighed and dried at 60 ºC for 24 h. A solution of 10 wt% SIBS was prepared by dissolving the polymer in 270 mL of methylene chloride under stirring at room temperature. The sulfonating agent, acetyl sulfate, was generated separately in an ice bath by mixing 20 mL of acetic anhydride and 12 mL of sulfuric acid in 180 mL of methylene chloride. The sulfonating agent solution was added to the 10 wt% SIBS solution and was aged under stirring at room temperature for 24 h to approximately yield 70% degree of sulfonation (DS). Following 24 h, 200 mL of methanol was added to isolate the sulfonated polymer by precipitation.[31] The sulfonated polymer was left at room temperature for 5 days to allow the solvents to evaporate. Finally, the sulfonated polymer was washed several times with DI water until it reached a pH of approximately 7.[31]

2.2.2. *Membrane casting*

Sulfonated SIBS membranes were prepared by the solvent casting method over polytetrafluoroethylene (PTFE) Petri dishes at room temperature.[28] Approximately 3 g of sulfonated SIBS were dried at 60 ºC for 24 h. A solution of 5 wt% sulfonated SIBS was prepared by dissolving the sulfonated polymer in a mixture of 85% toluene and 15% hexyl alcohol.[27] The mixture was stirred at room temperature for 24 h to ensure complete dissolution of the sulfonated polymer and transferred to a PTFE Petri dish to allow the solvents to evaporate and the membranes

to thermodynamically self-assemble. To ensure solvent residues were completely evaporated, the membrane was dried at 60 ºC for 24 h.

2.2.3. *Counter-ion substitution*

Sulfonated SIBS membranes were dried at 60 ºC for 24 h. Individually, the membranes were immersed in 25 mL of a 1.0 M aqueous solution of $CuCl_2$ and $FeCl_3$ salts to allow the Cu^{2+} and Fe^{3+} counter-ions exchange, respectively. When the exchange reaction was accomplished, the membranes were removed from the immersed solution and washed with DI water.

2.3. Materials characterization

2.3.1. *Elemental analysis*

Elemental analysis (EA) of sulfonated SIBS were performed by Atlantic Microlab (Norcross, GA) to quantitatively determine the percent by weight of carbon, hydrogen, and sulfur atoms. Equation 1 was used to obtain the mole percent of sulfonation,

$$Degree\ of\ Sulfonation = \frac{S}{C} \times 100\ \% \quad (1)$$

where S and C represent the sulfur and carbon in sulfonated polystyrene, respectively.[27] In order to perform the sulfonation percent calculation, it was assumed that the carbon in sulfonated polystyrene represents the 30 wt% of the total carbon present in SIBS.

2.3.2. *Ion exchange capacity*

Ion exchange capacity (IEC) of sulfonated SIBS is defined as milli-equivalent of sulfonic acid exchanged groups per gram of dry membrane (mequiv./g) and was determined via titration in

accordance to the procedure reported by Avilés-Barreto.[28,32,33] A sulfonated SIBS membrane was left in 25 mL of a 1.0 M NaCl solution for 24 h. Once the membrane was removed, the immersed solution was analyzed with a 0.1 M NaOH solution and phenolphthalein as indicator. IEC calculations were performed using equation 2,

$$IEC = \frac{C_{NaOH} \times V_{NaOH}}{m_{dry}} \qquad (2)$$

where, C_{NaOH}represents the concentration of NaOH, V_{NaOH} equals the volume of $NaOH$ used in the titration and m_{dry} equals the initial mass of the dry membrane.[32,33]

2.3.3. *Fourier transform infrared spectroscopy*

Fourier transform infrared spectroscopy (FTIR) was used to confirm the presence of sulfonic acid groups after the functionalization was achieved. Prior FTIR analysis, sulfonated SIBS membranes were dried at 60 ºC for 24 h. All transmittance spectra encompassed wavenumbers from 600 to 4000 cm^{-1} and were collected using 100 scans at 4 cm^{-1} of resolution with an Alpha's Platinum-ATR, manufactured by Bruker.

2.3.4. *Thermogravimetric analysis*

Thermogravimetric analysis (TGA) were performed by Edwards Life Sciences (Añasco, PR) following ASTM E1131-08(2014) international standard to evaluate the thermal stability of sulfonated SIBS membranes. Each membrane of approximately 10 mg, was heated from 30 ºC to 700 ºC at a constant ramp rate of 10 ºC/min in a nitrogen atmosphere.

2.3.5. *Small angle X-ray scattering*

Small angle X-ray scattering (SAXS) was used to measure interstitial (Bragg) distances, shape and size of the ionic domains present in sulfonated SIBS. Sulfonated SIBS membranes were dried at 60 ºC for 24 h and then placed on a paste cell in which a SAXS pattern was collected within 60 s. All measurements were performed using line-collimation with a Cu Kα X-ray source at 25 ºC in a SAXSpace modular nanostructured analyzer, manufactured by Anton Paar (Graz, Austria). The wavelength of the X-ray radiation was 1.54 Å and the sample-to-detector distance was near 0 nm. SAXSquant^{TM} software package was used to process the pattern collected and develop intensity profiles as a function of scattering vector at approximately 30 nm of resolution.[34]

2.3.6. *Atomic force microscopy*

Atomic force microscopy (AFM) high resolution images were obtained to visualize fine morphological features of sulfonated SIBS membranes. Intermittent contact mode, typically referred as AC mode, was employed for all AFM analysis in a 5500 Scanning Probe Microscope, manufactured by Agilent Technologies, Inc. (Palo Alto, CA). Phase images were obtained using a Point Probe Plus / Non-Contact / High Frequency tip (PPP-NCH-10, Keysight) with a nominal force constant of 42 N/m, tip length of 125 μm and a tip thickness of 4 μm. Using a reflective Au side, one scan per membrane was performed at 256 points/lines resolution at a speed between 1.7 to 1.9 lines/second (ln/s).

2.3.7. *Water uptake*

Water uptake (WU) measurements were performed to determine the water absorption capacity of sulfonated SIBS membranes when these are immersed in DI water. Sulfonated SIBS

membranes were dried at 60 ºC for 24 h and then immersed in 25 mL of deionized water at room temperature. Each membrane was weighed at different intervals of time for 24 h. The water absorption capacity percent was obtained using the following equation:

$$WU = \frac{W_{wet} - W_{dry}}{W_{dry}} \times 100\ \% \qquad (3)$$

where W_{wet} and W_{dry} represent the weights of the hydrated and dried membrane, respectively.[27,32]

2.3.8. *Instrumental neutron activation analysis*

Instrumental neutron activation analysis (INAA) was performed by Elemental Analysis, Inc. (Lexington, KY) to quantitatively determine a mole ratio between Cu^{2+} and Fe^{3+} counter-ions and sulfonic acid groups present in sulfonated SIBS membranes exchanged with cupric and ferric ions, respectively.

2.4. Antibacterial performance

2.4.1. *Protocol for the antibacterial analysis in batch conditions*

Antibacterial evaluations were performed in batch conditions by immersing a fragment of a membrane in the hydrated state in a water sample of 100 mL contained in a sterilized polypropylene vial. The vial was placed on top of an orbital shaker (GMI 8194-10-0990) to maintain a uniform agitation of 80 rpms for 10 min. Once the membrane was removed, the immersed solution was diluted in a phosphate buffer. The diluted solution was tested using the membrane filtration (MF) method with a 0.45 µm Millipore-size filter (Advantec MFS A045H047W) that was aseptically removed from the filter base, placed onto MI or mEI Agar and incubated for 24 h for the detection and enumeration of *E. coli* and *Enterococci*, respectively.[35,36]

The composition of MI and mEI Agar are presented in Table A.1 and Table A.2 shown in Appendix A, respectively.

2.4.2. *Membrane exposition using the membrane filtration experimental setup*

Instead of the Millipore-size filter, a fragment of approximately 50 mm diameter hydrated sulfonated SIBS membrane was placed on the filter base of the MF system. An air-tight seal was produced by a vacuum pump (Gast DOA-P104-AA) to allow holding water on top of the membrane for 10 min. Similar to that of batch conditions, the Millipore-size filter was removed, placed onto the desired Agar and incubated for 24 h.

2.4.2.1. Preparation of bacterial suspensions from certified bacterial strains

E. coli (ATCC 25922) and *E. fecalis* (ATCC 29212) bacterial strains where obtained from the Department of Biology, University of Puerto Rico at Mayagüez. For each culture, a representative number of colonies was collected using a disposable inoculation loop and placed in 9 mL of diluent to prepare a pellet. The solution was centrifuged (Corning® LSE™ Compact Centrifuge 6755) for 10 min at 3000 rpms; the centrifugation process was done three times. Finally, the pellet was dissolved in 200 mL of diluent and the initial concentration was determined after 24 h of incubation.

2.4.2.2. Water quality parameters

The sampling water was monitored for the temperature, pH, turbidity and dissolved oxygen. These quality parameters were measured with a pH portable meter (Oakton WD-35613-

50), a portable turbidimeter (Oakton WD-35635-00) and a hand-held dissolved oxygen meter (Oakton WD-35640-20).

2.4.3. *Interpretation of antibacterial analysis results*

After overnight incubation, the total number of colonies per plate is determined by visual inspection. Then, a cell density, which represents the number of pathogenic bacteria per 100 mL, is calculated with the following equation,

$$pathogenic\ bacteria/100\ mL\ = \frac{number\ of\ colonies}{volume\ of\ sample\ filtered\ (mL)} \times\ 100 \quad (5)$$

where the results obtained are reported as colony forming units (CFU) per 100 mL (CFU/100 mL).[35,36] These results are used to calculate the percentage of viable cells after the treatment. The percent of cell viability is obtained with the following equation,

$$cell\ viability = \frac{living\ pathogenic\ bacteria/100\ mL}{total\ pathogenic\ bacteria/100\ mL} \times\ 100 \quad (6)$$

In this work, cell viability results are presented as a representation of the efficiency of sulfonated SIBS to inactivate pathogenic bacteria.[37]

3 Experimental results and discussion

3.1. Materials characterization

3.1.1. *Incorporation of the sulfonic acid groups*

Sulfonation is an electrophilic substitution reaction where a sulfonic acid group is chemically attached to the aromatic ring of an organic compound.[38] In certain cases, hindrances due to the increase in steric effects and repulsion arise when the sulfonic acid groups are incorporated into the aromatic ring.[38] Sulfonation of aromatic compounds may results in the mono-substitution of the sulfonic acid groups at the *para*-position of the aromatic ring, as shown in Figure 1.[38] In general, the overall content and distribution of sulfonic acid groups may depend on the concentration of polymer in a thermodynamically favorable solvent and the choice of the sulfonating agent.[32,38,39] For instance, sulfonation of block copolymers can be achieved by using acetyl sulfate as the sulfonating agent in chlorinated solvents such as methylene chloride.[39] According to the procedure reported by Avilés-Barreto, acetyl sulfate is generated from acetic

anhydride and sulfuric acid as shown in Figure 2, accompanied by the formation of acetic acid as a byproduct.[28]

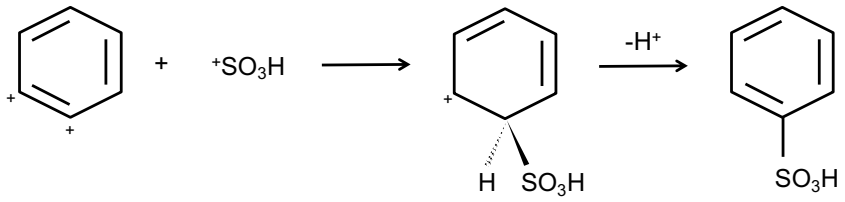

Figure 1. Incorporation of the sulfonic acid group in the *para*-position of the aromatic ring.

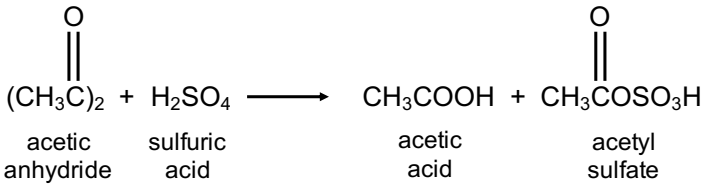

Figure 2. Acetyl sulfate generated from acetic anhydride and sulfuric acid reaction.

Taking poly(styrene-isobutylene-styrene) (SIBS) with 30% polystyrene, a sulfonic acid group may be randomly attached in the *para*-position of the aromatic ring present in the polystyrene block, as seen in Figure 3.[28,38] The incorporation of sulfonic acid groups into SIBS can be confirmed using FTIR and TGA analysis.[28,31,32,39,40] While vibrational spectroscopy analysis is employed to describe the functionalization achieved, with thermogravimetric analysis it is possible to measure the decomposition of the sulfonated polymer subjected to a heating rate in a controlled atmosphere.[41,42]

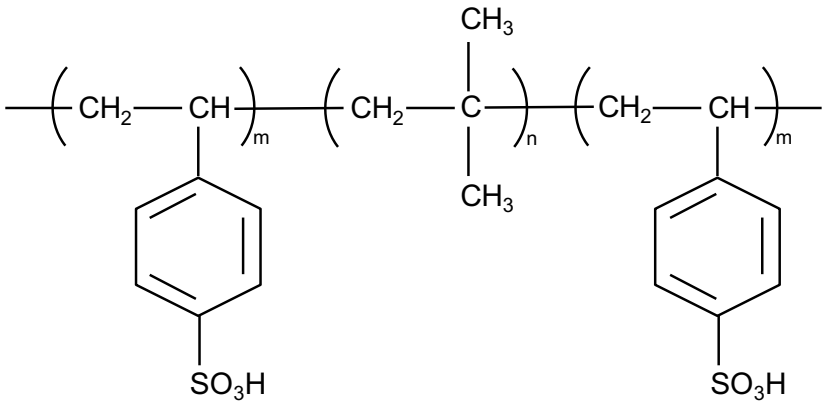

Figure 3. Sulfonic acid groups incorporated into poly(styrene-isobutylene-styrene).

Spectroscopy analysis was performed to provide a description of important characteristic bands associated with the sulfonic acid groups incorporated in SIBS. FTIR transmittance spectra for sulfonated SIBS at four different degrees of sulfonation are presented in Figure 4. The incorporation of sulfonic acid groups into SIBS is characterized by two strong vibration bands at 1070-1030 cm^{-1} and 1200-1140 cm^{-1} for the sulfonate group symmetric and asymmetric stretching vibrations, respectively.[41,43] Usually, the band due to the asymmetric stretching vibration of the sulfonate group is broad and with shoulders while the band due to the symmetric stretching vibration of the sulfonate group is sharper with shoulders.[27,43,44] Besides the stretching modes of vibration of the sulfonate group, sulfonated SIBS have a band at 1290-990 cm^{-1} and at 1300-1050 cm^{-1} due to the attachment of the sulfonate group into the aromatic ring and the mono-substitution of the sulfonate group in the *para*-position of the aromatic ring, respectively.[27,28,31] In general, most of the aromatic ring vibrational modes are unaffected by the attachment of functional groups with exception of the in-plane bending vibration mode of the aromatic ring.[41] The in-plane bending vibration mode of the aromatic ring due to the mono-substitution of the sulfonate group into the *para*-position of the aromatic ring is sensitive to the electronic properties of the sulfonate group attached.[27,41]

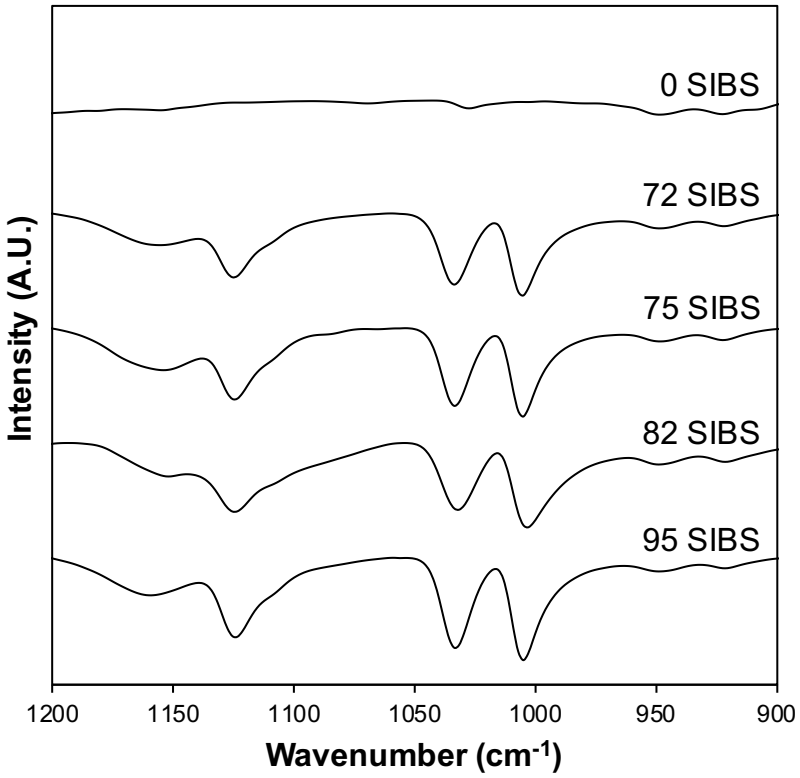

Figure 4. FTIR transmittance spectra for sulfonated SIBS at different degrees of sulfonation.

The FTIR vibrational stretching bands wavenumbers for sulfonated SIBS are summarized in Table 1. While vibration bands such as the asymmetric vibration of the sulfonate group and the attachment of the sulfonate anion into the aromatic ring remain unchanged, the symmetric vibration of the sulfonate group and the mono-substitution in the *para*-position of the aromatic ring band show a minor displacement. Fundamental vibrational stretching bands of sulfonated polymers are typically environmentally sensitive and changes in atmospheric moisture may affect its measurements.[41]

Table 1. FTIR vibrational stretching bands of sulfonated SIBS at different degrees of sulfonation.

	FTIR vibrational stretching bands wavenumbers (cm^{-1})			
Sample	asymmetric vibration of the sulfonate group	sulfonate anion attached to the aromatic ring	symmetric vibration of the sulfonate group	*mono*-substitution in the *para*-position of the aromatic ring
72 SIBS	1156	1125	1034	1006
75 SIBS	1156	1125	1034	1006
82 SIBS	1156	1125	1032	1004
95 SIBS	1156	1125	1033	1005

On the other hand, the thermal degradation of sulfonated SIBS was evaluated using TGA analysis. The thermal curves of sulfonated SIBS at four different degrees of sulfonation are presented in Figure 5. As seen in Figure 5, each thermal curve shows a descending shape which is characteristic of a weight loss suggesting polymer degradation.[42,45] The degradation of sulfonated SIBS shows three stages while a single-stage degradation at approximately 432 ºC corresponding to the breakdown of the polymer backbone has been reported for SIBS.[28,32,46] In the thermal curves seen in Figure 5, a drying step corresponding to the loss of atmospheric moisture is observed at the beginning near 50-200 ºC, followed by the decomposition of the sulfonic acid groups at 200-350 ºC and the thermal degradation of the polymer backbone at 370-430 ºC towards the end.[28,32,42,46]

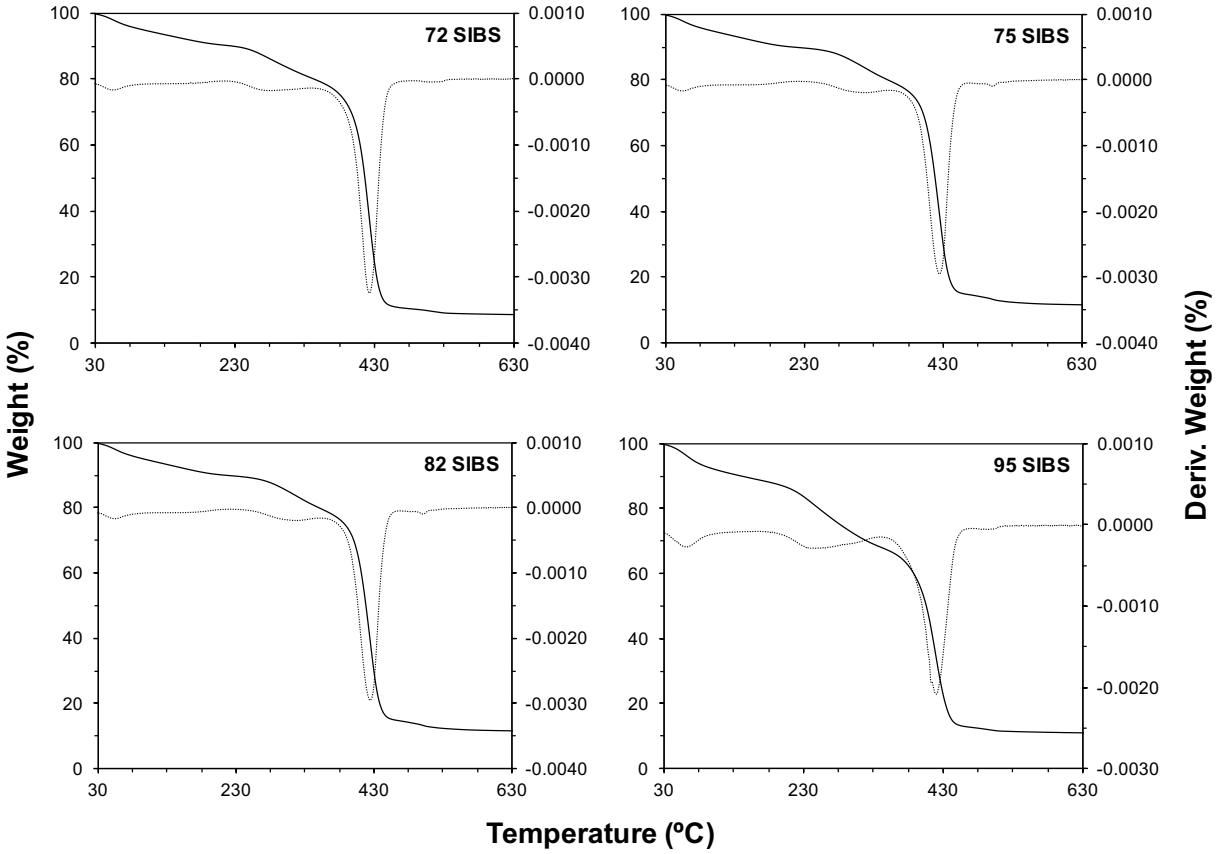

Figure 5. Thermogravimetric analysis of sulfonated SIBS at different degrees of sulfonation.

The thermal degradation temperatures of sulfonated SIBS at four different degrees of sulfonation, obtained from the peaks shown in the first derivative curves, are summarized in Table 2. As seen in Table 2, the rate of decomposition of the sulfonic acid groups varies with the degree of sulfonation perhaps due to variations in the asymmetry of the sulfonated SIBS structure.[32,46,47] However, regardless of the specific degradation temperature, a complete decomposition of the sulfonic acid groups was obtained while the thermal degradation of the polymer backbone remained practically the same for each degree of sulfonation.[28,32,46] Nevertheless, two steps overlap in the thermal transition of the polymer backbone degradation since the decomposition of the polystyrene at 420 ºC and isobutylene at 455 ºC monomers cannot be individually identified.[28,40]

A better separation of the monomer decomposition could be achieved with a different heating rate or sample weight.[42,45]

Table 2. Thermal degradation temperatures for sulfonated SIBS at different degrees of sulfonation.

	Degradation temperatures (ºC)		
Sample	atmospheric moisture	decomposition of sulfonic acid groups	thermal degradation of the polymer backbone
72 SIBS	57	272	422
75 SIBS	56	310	423
82 SIBS	62	261	422
95 SIBS	64	238	421

Although FTIR and TGA analysis have provided fundamental evidence for the incorporation of sulfonic acid groups into SIBS, a deeper insight into the structure, size and, distribution of the aggregates can be helpful to explain the differences in the sulfonated polymer as the degree of sulfonation increases. The means to characterize the structural features of sulfonated SIBS brings useful information to build an understanding of the ionic domains and provide a broad overview of the SIBS sulfonation synthesis, morphology, and properties. These materials characterization techniques include scattering methods and proximal probe techniques.

3.1.2. *The effect of degree of sulfonation*

The incorporation of sulfonic acid groups into SIBS was achieved at different degrees of sulfonation. When the sulfonating agent was added in a minor proportion (25 mL of acetic anhydride, 14 mL of sulfuric acid) and the sulfonation was carried out at room temperature for 24 h, approximately 70% degree of sulfonation was obtained. In the other hand, 95% degree of

sulfonation was obtained when the sulfonating agent was added in a higher proportion (50 mL of acetic anhydride, 28 mL of sulfuric acid) and the reaction time was increased to 48 h.

The percent by weight of carbon, hydrogen and sulfur atoms in the sulfonated SIBS was determined by elemental analysis and accordingly the calculation of the degree of sulfonation was obtained using equation 1. Similarly, ion-exchange capacity was determined for sulfonated SIBS via titration to provide an estimate of the number of ion exchangeable sites in the sulfonated polymer.[32,33] Moreover, this method allowed the calculation of the degree of sulfonation using equation 2.[32] The results of ion exchange capacity as a function of the degree of sulfonation are presented in Figure 6. The values of ion exchange capacity, with exception of 95% degree of sulfonation, are continuously increasing. As seen in Figure 6, the ion exchange capacity for the highest degree of sulfonation obtained dropped and a maximum ion exchange capacity value of 1.82 mequiv./g was achieved for 85% degree of sulfonation.

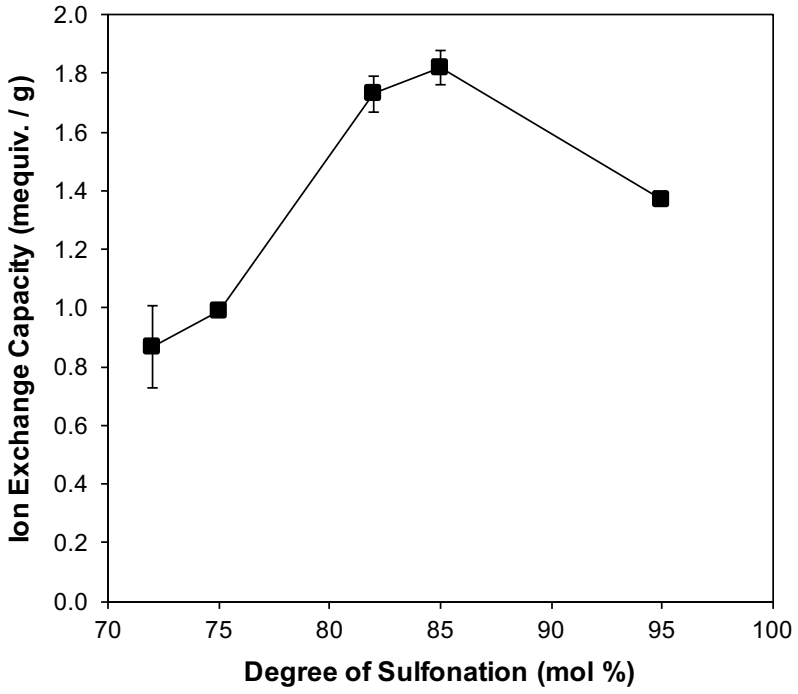

Figure 6. Ion exchange capacity as a function of degree of sulfonation.

Along with the incorporation of sulfonic acid groups into SIBS, the formation of ionic domains was promoted, followed by a phase separation of ion-rich aggregates within sulfonated SIBS.[28,31,39,47] Significantly influenced by the degree of sulfonation, the ionic domains act as very stable crosslinks and can grow due to electrostatic interactions until the formation of ionic channels is promoted.[28,38,47] The size and distribution of ionic domains across the sulfonated polymer increase with a higher content of sulfonic acid groups.[47] Although increasing the degree of sulfonation increases the ion exchange capacity, for the highest degree of sulfonation obtained, the possibility of reaching available ion-exchangeable sites became restricted due to mass-transfer limitations; and, the ion exchange capacity decreased because continuous ionic channels arise from the interconnection of ionic domains.[27,28,47]

The ionic domains phase separates into small ion-rich aggregates giving rise to the formation of micro-domains in the structure of sulfonated SIBS.[48] The morphology of the micro-domains can be measured with elastic scattering methods in the small angle region such as SAXS.[39] In SAXS, the collection of the elastic interactions detected are associated with variations in electronic densities from the different interfaces present within the sample.[49] Accordingly, the scattering intensity I(q) is measured as a function of the scattering vector q to provide I(q) versus q scattering profiles.[50] The scattering intensity is defined as the Fourier Transform of the correlation of electronic densities corresponding to the probability of finding a scattered with respect to another scattered; and, is given in absolute intensities to exclusively eliminate any dependence of the measurement with the sample thickness.[49] The magnitude of the scattering vector is defined as,

$$q = \frac{4\pi \sin(\theta)}{\lambda} \qquad (7)$$

where 2θ represents the scattering angle and λ the wavelength of the incident beam.[50]

Scattering profiles collected for sulfonated SIBS at different degrees of sulfonation, as seen in Figure 7, have been used to deduce fundamental characteristic of the ionic domains. In the SAXS profile of SIBS, a small-angle upturn is observed, followed by a broad peak at wide angles while two peaks are simultaneously evidenced in the SAXS profiles obtained for sulfonated SIBS. For the SAXS profiles of sulfonated SIBS, the first peak located at smaller angles represents the ionomer peak while the second broad peak located at wide angles remains stable, regardless of the degree of sulfonation.

In SAXS, the ionomer peak evidences the incorporation of the sulfonic acid groups separated by long isobutylene sequences, as well as the existence of well-defined shapes that give rise to micro-phase separation.[31,49–51] On the other hand, at higher angles, it is possible to obtain information about smaller features located in the same polystyrene block.[49,50] Thus, the broad peak at wide angles observed for sulfonated SIBS at different degrees of sulfonation suggests the existence of short intramolecular distances between ionic domains along the polystyrene block of the sulfonated polymer.[50]

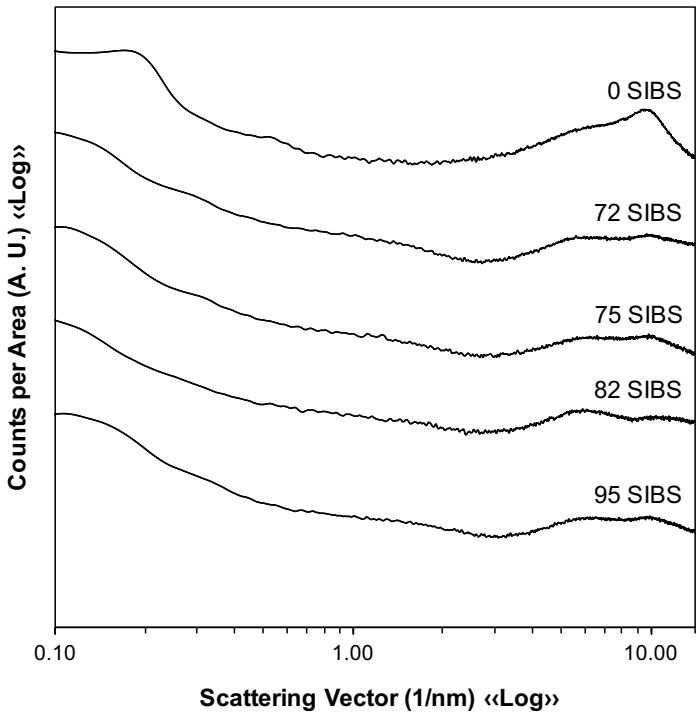

Figure 7. SAXS profiles for sulfonated SIBS at different degrees of sulfonation.

The scattering vector at the maximum intensity (q_{peak}) is related to the distance (d_{Bragg}) between the assembled sulfonic acid groups by using Bragg's law, as shown in equation 6.[28,34,39,52]

$$d_{Bragg} = \frac{2\pi}{q_{peak}} \qquad (6)$$

The interstitial distance results for sulfonated SIBS at different degrees of sulfonation are summarized in Table 3. As seen in Table 3, the interstitial distance reaches a maximum value when increasing the degree of sulfonation, suggesting that the distance between ionic domains increases.[28,52] However, even when Bragg's Law does not measure a periodic variation in electron density when a difference between the matrix and the ionic domains within sulfonated SIBS exists, the interstitial distance may represent the size of the ionic nanochannels promoted by the interconnection of the ionic domains.[34,39,53] The ionomer peak for sulfonated SIBS at 82% degree of sulfonation showed the largest interstitial distance perhaps due to the impact of the great electron

density of the ionic domains.[49] This may have contributed to a more destructive interface and weaker scattering intensity.[49] Furthermore, this feature can be related to the increasing IEC obtained for sulfonated SIBS at 82% degree of sulfonation; recall Figure 6.[50]

Table 3. Interstitial distance for sulfonated SIBS at different degrees of sulfonation.

Sample	Scattering Vector (1/nm)	Interstitial Distance (nm)
0 SIBS	0.196	32.06
72 SIBS	0.139	45.20
75 SIBS	0.138	45.53
82 SIBS	0.129	48.71
95 SIBS	0.151	41.61

Moreover, the analysis of SAXS profiles allows the use of a form factor describing the shape of the ionic domains.[34,39] In a double-logarithmic plot, the slope of the form factor at small angles can be calculated.[34] Accordingly, a preliminary classification into a spherical structure of SIBS was determined while a lamellar self-assembled structure with rough interfaces of the ionic domain was obtained for sulfonated SIBS, regardless of the degree of sulfonation.[34,47,49] Thus, the results associated with the shape of the ionic domains suggested that at high degrees of sulfonation, the morphology of sulfonated SIBS does not change.[39]

For sulfonated SIBS at different degrees of sulfonation, a non-linear dependence was observed from the Guinier's approximation, thus suggesting the presence of aggregation in sulfonated SIBS.[34] Consequently, a polydispersity analysis was performed, which results suggested that the ionic domains within sulfonated SIBS exhibited the same lamellar shape but with different sizes.[34,49] Therefore, since the particles may have different sizes across the sample,

the SAXS profiles shown in Figure 7 represent an average scattering pattern of sulfonated SIBS.[34,49]

The SAXS results obtained about the structure of the ionic domains serve as a reference for the morphological studies employing AFM.[48] Microphase separation, usually well-defined in a phase image, can be observed using AFM.[54] However, for sulfonated SIBS, a cluster-like structure is not clearly visible in the phase images presented in Figure 8. Experimental and theoretical evidence indicates that ionic domains undergo micro-phase separation into hydrophilic and hydrophobic domains, represented by lighter and darker regions, respectively.[32,48] This phase contrast is due to the fact that at room temperature, the polystyrene is in a glassy state and matches the higher areas while isobutylene is in a rubber-like state.[54]

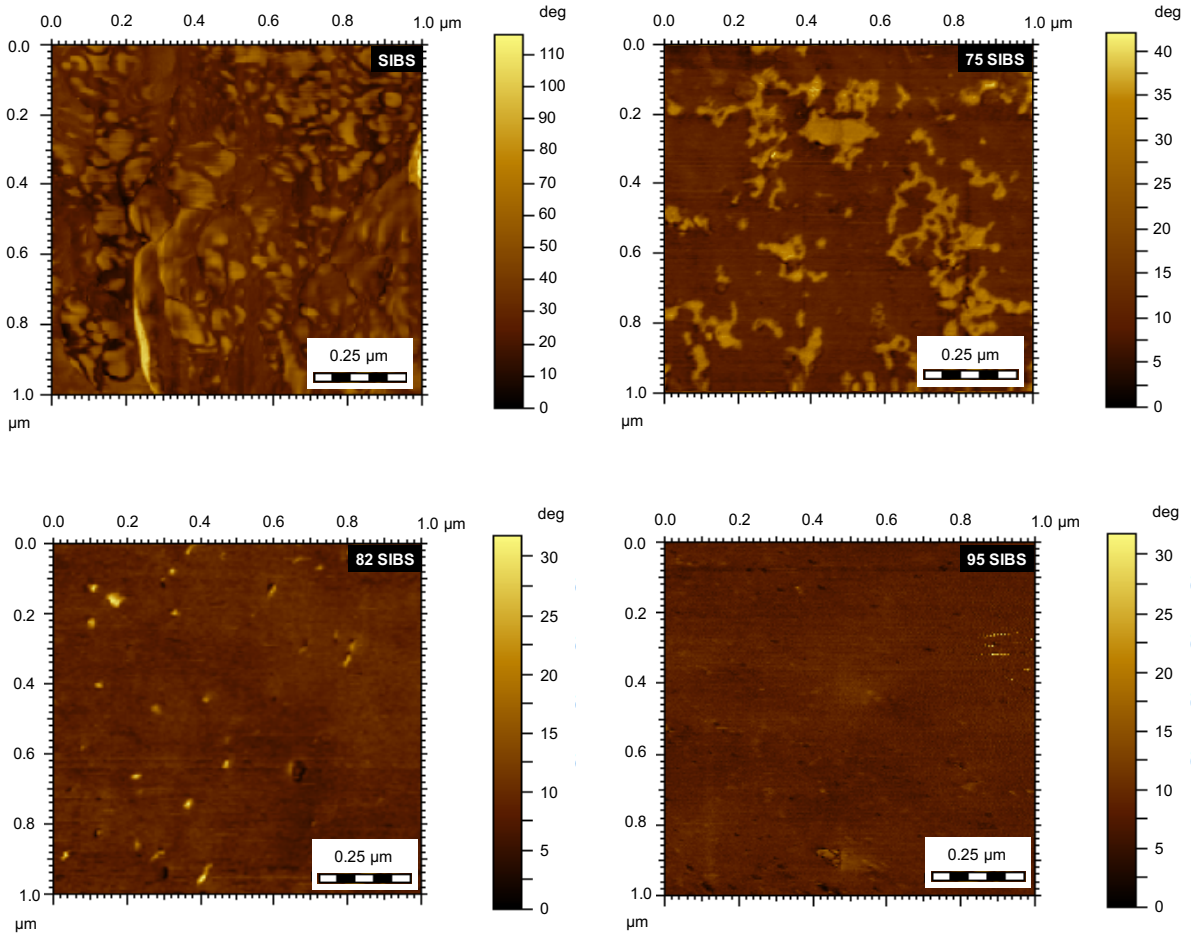

Figure 8. Phase images for sulfonated SIBS at different degrees of sulfonation.

The surface roughness of sulfonated SIBS was obtained using the AFM.[55] The roughness of sulfonated SIBS was determined by taking the arithmetic mean of the height from the surface of each membrane.[55] The values of roughness for sulfonated SIBS at three different degrees of sulfonation are summarized in Table 4. As seen in Table 4, a significant decrease in roughness was obtained for sulfonated SIBS with respect to SIBS. A maximum roughness value of 9.41 nm was achieved for 82% degree of sulfonation; and, for 75% and 95% degree of sulfonation, a similar value for the roughness was obtained. However, the phase images of sulfonated SIBS at different degrees of sulfonation are quite different in appearance. As seen in Figure 8, the structural features

of sulfonated SIBS are minimized as the degree of sulfonation increases.[32] Accordingly, while the degree of sulfonation increased, a smooth-like appearance with fewer imperfections is seen after the membrane casting process was completed.[56]

Table 4. Roughness for SIBS and sulfonated SIBS at three different degrees of sulfonation.

Sample	Roughness (nm)
0 SIBS	31.52
75 SIBS	4.03
82 SIBS	9.41
95 SIBS	4.39

Sulfonation and the techniques used to characterize the sulfonated polymer can be used to elucidate the properties attained by the incorporation of the sulfonic acid groups. For instance, both the degree of sulfonation and the structure of the ionic domains are two important factors in determining the water absorption capacity of a sulfonated polymer.[47] Hence, achieving such lamellar structure of the ionic domains after the incorporation of the sulfonic acid group resembles in the enhancement of the water absorption capacity of SIBS.[32,39,47,48] Typically, SIBS have a low tendency to absorb water but sulfonated SIBS at different degrees of sulfonation reaches extremely high values of water absorption, as presented in Figure 9.[48]

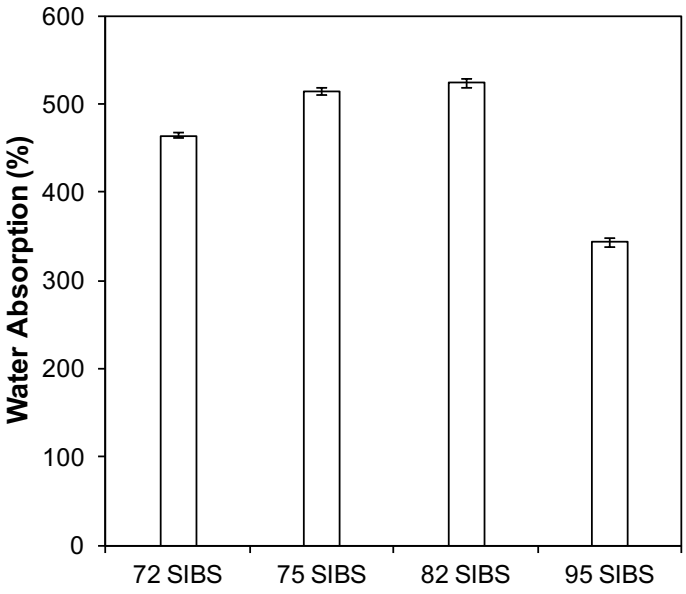

Figure 9. Water absorption capacity of sulfonated SIBS at different degrees of sulfonation.

The existence of sulfonic acid groups in a sulfonated polymer gives rise to strong interactions with water perhaps due to the capability of successfully maintaining the water within ionic domains.[47] Also, a fully-hydrated sulfonated SIBS membrane may double its dimensions while the number of sulfonic acid groups remains unchanged.[39]

Furthermore, sulfonated SIBS can be used to perform counter-ions exchange reactions. For instance, Cu^{2+} and Fe^{3+} counter-ions can be easily exchanged within ion-exchangeable sites present in sulfonated polymers.[28,57] However, the incorporation of counter-ions in a sulfonated polymer may lead to changes in the chemical, thermal and structural behaviors of the polymer. Hence, the focus is on identifying and closely study the effects of the counter-ions within the sulfonated polymer.

3.1.3. *The effect of counter-ion substitution*

Sulfonated SIBS can be modified by allowing the neutralization of ion-exchangeable sites within the sulfonated polymer with counter-ions, such as Cu^{2+} and Fe^{3+}. The incorporation of these species is achieved following an exchange reaction where a counter-ion is electrostatically attracted and then replaced by the H^+ present in the sulfonic acid groups.[28,39,58]

Typically, a sulfonated SIBS membrane is immersed in a solution of copper chloride ($CuCl_2$) or ferric chloride ($FeCl_3$) to allow the substitution of Cu^{2+} and Fe^{3+} counter-ions, respectively. Although this method is successfully employed for the exchange reaction, the number of cations associated with the sulfonic acid groups is different for each counter-ion, and it is expected to remains the same regardless of the degree of sulfonation.[28] It has been proven by INAA that an average ratio of one metal every two sulfonic acid groups are obtained for divalent cations.[28] However, evidence from INAA experimental results shown in Table 5, indicates that, whether is Cu^{2+} or Fe^{3+}, more than two sulfonic acid groups are associated with the counter-ions exchanged in sulfonated SIBS. These results considerably increase the number of sulfonic acid groups that became available for the exchange reaction and can, therefore, be used to this end.[39] Nevertheless, through the INAA analysis performed, it is not assured that the counter-ions were exchanged with the total sulfonic acid groups present.

Table 5. Mole ratio between counter-ions and sulfonic acid groups.

Sample	Sulfonic acid groups per counter-ion
82 SIBS Cu	3
95 SIBS Cu	3
72 SIBS Fe	3
75 SIBS Fe	4
82 SIBS Fe	4
95 SIBS Fe	4

In solution, some dissociated counter-ions diffuse along and between the sulfonated polymer to either bridge or repel the sulfonate groups with each other.[39] Furthermore, counter-ions can associate to develop cross-linked ionic clusters.[24,48,57] The diffusion path and its tortuosity depend on the extent of swelling, defined by the ion exchange capacity and, the organization of the sulfonic acid groups.[39]

The sulfonic acid groups react with the counter-ions to the point that the exchange slows down as the reaction proceeds due to the steric effects caused by the substituted neighboring groups.[38,39] Also, since this reaction may result in the formation of sulfates and metal oxides, the metal oxides may also be responsible for slowing down the reaction since the surface of the counter-ions may become unreactive in presence of oxides.[38,39]

It has been found that the exchange of counter-ions leads to observable alterations of the sulfonation functionality.[28] The effect and role of counter-ions have been associated with characteristic features observed in the sulfonated polymer after the incorporation of sulfonic acid groups is achieved. Therefore, the characteristic features of the sulfonated polymer are used as a reference to show the effect of the counter-ions in the sulfonated polymer, thereby helping to

elucidate the chemical, thermal and structural modifications of the sulfonated polymer after the counter-ion substitution is achieved.

FTIR transmittance spectra for copper-exchanged and iron-exchanged sulfonated SIBS are presented in Figure 10. Although no additional bands are associated with the counter-ions exchanged in the sulfonated polymer, an increase in the overall intensity and a slight shift of the asymmetric stretching vibration of the sulfonate group band is observed for copper-exchanged and iron-exchanged sulfonated SIBS.[28,53] As seen in Figure 10, the asymmetric stretching vibration of the sulfonate group is thought to be dependent of counter-ion and that no observable shift can be seen for the remaining bands present in the FTIR spectra for copper-exchanged and iron-exchanged sulfonated SIBS.[28]

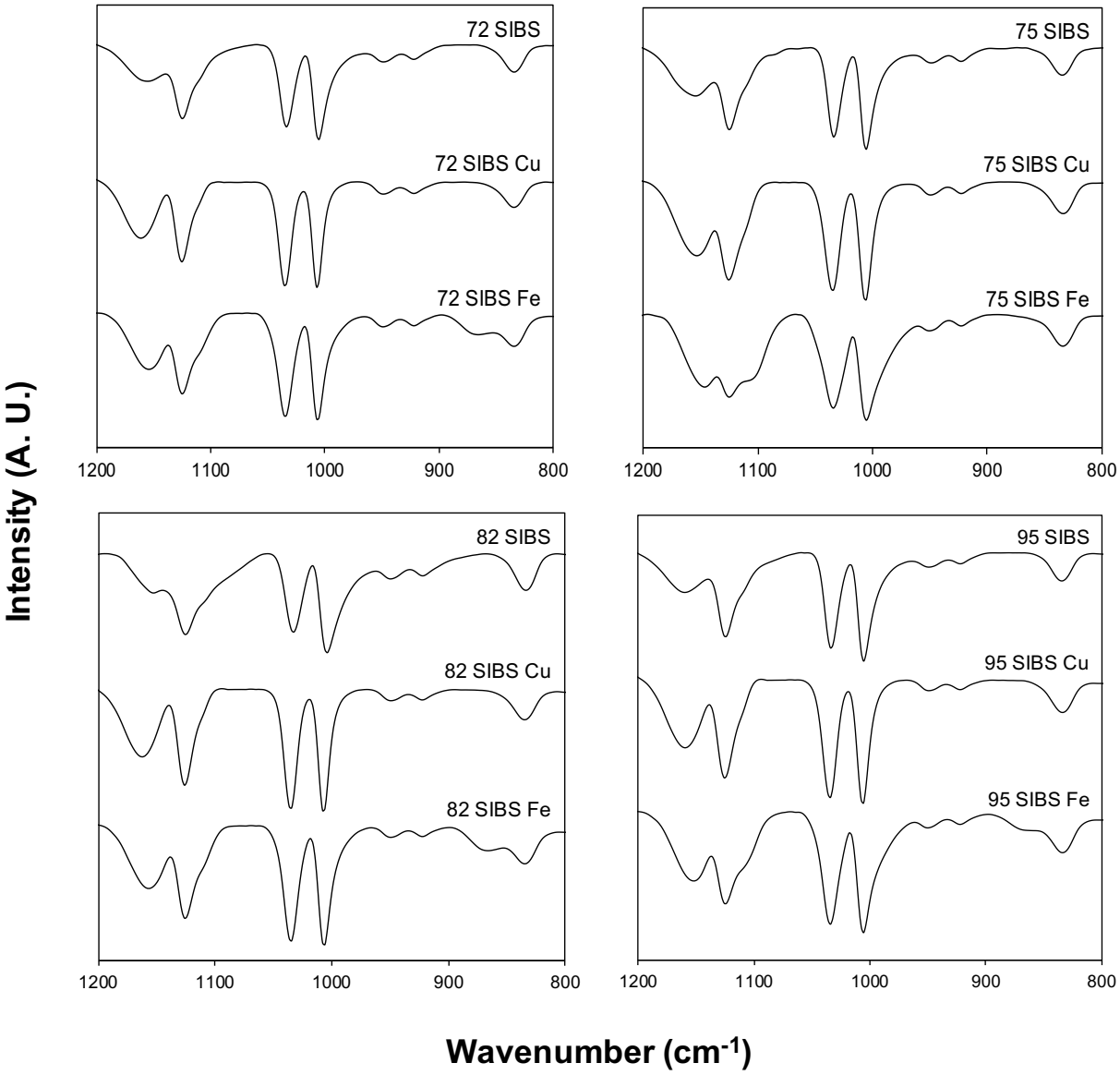

Figure 10. FTIR transmittance spectra for copper-exchanged and iron-exchanged sulfonated SIBS.

The FTIR vibrational stretching bands wavenumbers for copper-exchanged and iron-exchanged sulfonated SIBS are summarized in Table 6. In addition to the changes obtained for copper-exchanged sulfonated SIBS, the shoulder of the band due to the attachment of the sulfonate group into the aromatic ring in the iron-exchanged sulfonated SIBS is more defined.[44] Also, the

iron-exchanged sulfonated SIBS exhibits the appearance of an additional band in the FTIR transmittance spectra due to the possible presence of metal oxides from the Fe-O-Fe group.[24] The antisymmetric stretching vibration band of Fe-O-Fe at 870 cm^{-1} appeared for iron-exchanged sulfonated SIBS, regardless of the degree of sulfonation.[24,41,57] The exchange of Fe^{3+} with sulfonic acid groups can be associated with the formation of metal oxides from the Fe-O-Fe group although it has been reported that the counter-ions move across the sulfonated polymer and establish strong interactions with the sulfonic acid groups. [24,57] Species such as metal oxides from the Fe-O-Fe group may be in the surface of sulfonated SIBS or confined within the cross-linked ionic domains.[24,57]

Table 6. FTIR vibrational stretching bands wavenumbers for copper-exchanged and iron-exchanged sulfonated SIBS.

	FTIR vibrational stretching bands wavenumbers (cm^{-1})			
Sample	asymmetric vibration of the sulfonate group	sulfonate anion attached to the aromatic ring	symmetric vibration of the sulfonate group	*mono*-substitution in the *para*-position of the aromatic ring
72 SIBS	1156	1125	1034	1006
72 SIBS Cu	1162	1126	1035	1007
72 SIBS Fe	1155	1125	1035	1007
75 SIBS	1156	1125	1034	1006
75 SIBS Cu	1153	1125	1035	1006
75 SIBS Fe	1146	1125	1034	1005
82 SIBS	1156	1125	1032	1004
82 SIBS Cu	1162	1126	1035	1007
82 SIBS Fe	1156	1125	1035	1006
95 SIBS	1156	1125	1033	1005
95 SIBS Cu	1159	1125	1034	1006
95 SIBS Fe	1152	1125	1034	1006

Although we have only considered Cu^{2+} and Fe^{3+}counter-ions, from the FTIR spectra it can be speculated that Fe^{3+} exchange is preferable that the Cu^{2+} exchange in sulfonated SIBS.[24] This may be due to a stronger affinity between Fe^{3+} and the sulfonic acid groups compared to the Cu^{2+} counter-ion.[24]

The strong interactions between the counter-ions with the sulfonic acid groups influence the thermal behavior of the sulfonated polymer.[40] Accordingly, thermogravimetric analysis of copper-exchanged and iron-exchanged sulfonated SIBS was performed and the results are

presented in Figure 11. In general, the counter-ions thwarted the effect of the atmospheric moisture in the thermogravimetric analysis.[28] Consequently, the drying step corresponding to the loss of atmospheric moisture seen for sulfonated SIBS is not observed for copper-exchanged or iron-exchanged sulfonated SIBS. Regardless of the degree of sulfonation, copper-exchanged and iron-exchanged sulfonated SIBS showed two unique degradations at 200-390ºC and 480-530ºC that can be related to the decomposition of the sulfonic acid groups associated with the Cu^{2+} and Fe^{3+} counter-ions, respectively.[28,40] These degradations suggest that the interaction between the counter-ions and the sulfonic acid groups is stronger for iron-exchanged sulfonated SIBS than copper-exchanged sulfonated SIBS.[40] For instance, copper-exchanged sulfonated SIBS showed the lowest thermal stability perhaps due to its high electronegativity while iron-exchanged sulfonated SIBS improved the thermal stability of the sulfonated polymer.[28,40]

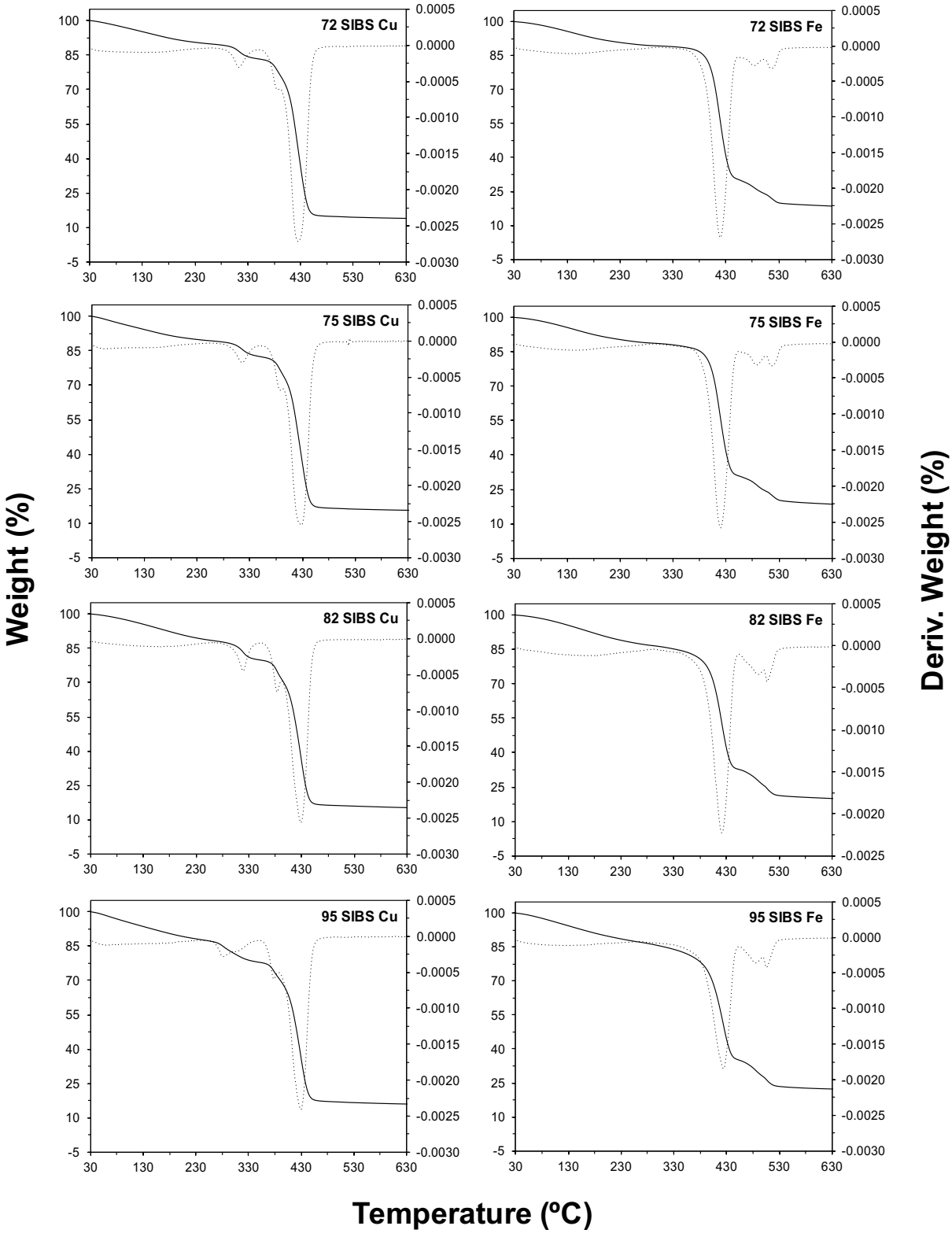

Figure 11. Thermal degradation of copper-exchanged and iron-exchanged sulfonated SIBS.

The thermal degradation temperatures of copper-exchanged and iron-exchanged sulfonated SIBS are summarized in Table 7. In general, the thermal degradation temperatures copper-exchanged and iron-exchanged sulfonated SIBS are slightly different from the temperatures of the sulfonated polymer; recall Table 2. Hence, for copper-exchanged and iron-exchanged sulfonated SIBS, a dependence on the counter-ion exchanged is observed for the thermal degradation of the polymer backbone. Similarly, the thermal decomposition of sulfonic acid groups depends very strongly on the counter-ions exchanged.[47] These observations suggest that a similar behavior for the decomposition of the sulfonic acid groups can be obtained, regardless of the counter-ion exchanged, but in different temperature regions.

Table 7. Thermal degradation temperatures of copper-exchanged and iron-exchanged sulfonated SIBS.

	Degradation temperatures (ºC)		
Sample	decomposition of sulfonic acid groups		thermal degradation of the polymer backbone
72 SIBS Cu	315	388	427
72 SIBS Fe	485	518	418
75 SIBS Cu	318	389	429
75 SIBS Fe	490	519	418
82 SIBS Cu	316	382	427
82 SIBS Fe	492	505	419
95 SIBS Cu	284	376	427
95 SIBS Fe	488	504	422

It has been suggested that the differences in degradation temperatures observed for copper-exchanged and iron-exchanged sulfonated SIBS could be related to differences in their structure.[40] In order to elucidate possible effects in the structure of the sulfonated polymer after counter-ion exchange, an evaluation of SAXS scattering profiles showed in Figure 12, was performed. It has been found that the ionomer peak for sulfonated SIBS exchanged with counter-ions is slightly different from the ionomer peak for sulfonated SIBS.[28,53] For copper-exchanged and iron-exchanged sulfonated SIBS, the lamellar self-assembled structure with rough interfaces and different sizes is preserved. Thus, the results suggest that the morphology of copper-exchanged and iron-exchanged sulfonated SIBS is mainly determined by that of the sulfonated polymer, although at the wide angles region is probably dependent on the counter-ion exchanged. The evaluation of the scattering profiles shown in Figure 12, suggests that the broad peak at wide angles observed for sulfonated SIBS behaves differently for copper-exchanged and iron-exchanged sulfonated SIBS. For copper-exchanged sulfonated SIBS, two broad peaks in the wide angles region can be visible.[34] Accordingly, the interstitial distance for each peak was calculated using equation 6 and the results are summarized in Table 8. As seen in Table 8, the interstitial distance of the first peak decreases as the degree of sulfonation increases, while the interstitial distance of the second peak remains the same. The appearance of these two broad peaks suggests that there exists a loose binding between Cu^{2+} and the sulfonic acid groups, thereby increasing the electron density contrast between the ionic domains and the hydrophilic region in the copper-exchanged sulfonated SIBS.[24,34,39,53] This feature remains invisible for iron-exchanged sulfonated SIBS. Also, as the degree of sulfonation increases, the peak at wide angles for iron-exchanged sulfonated SIBS is difficult to identify. Thus, it is possible that scattering in the aggregation of the cross-linked

ionic clusters is lost perhaps due to strong interactions between Fe^{3+} and the sulfonic acid groups through the iron-exchanged sulfonated SIBS.[24,39,40]

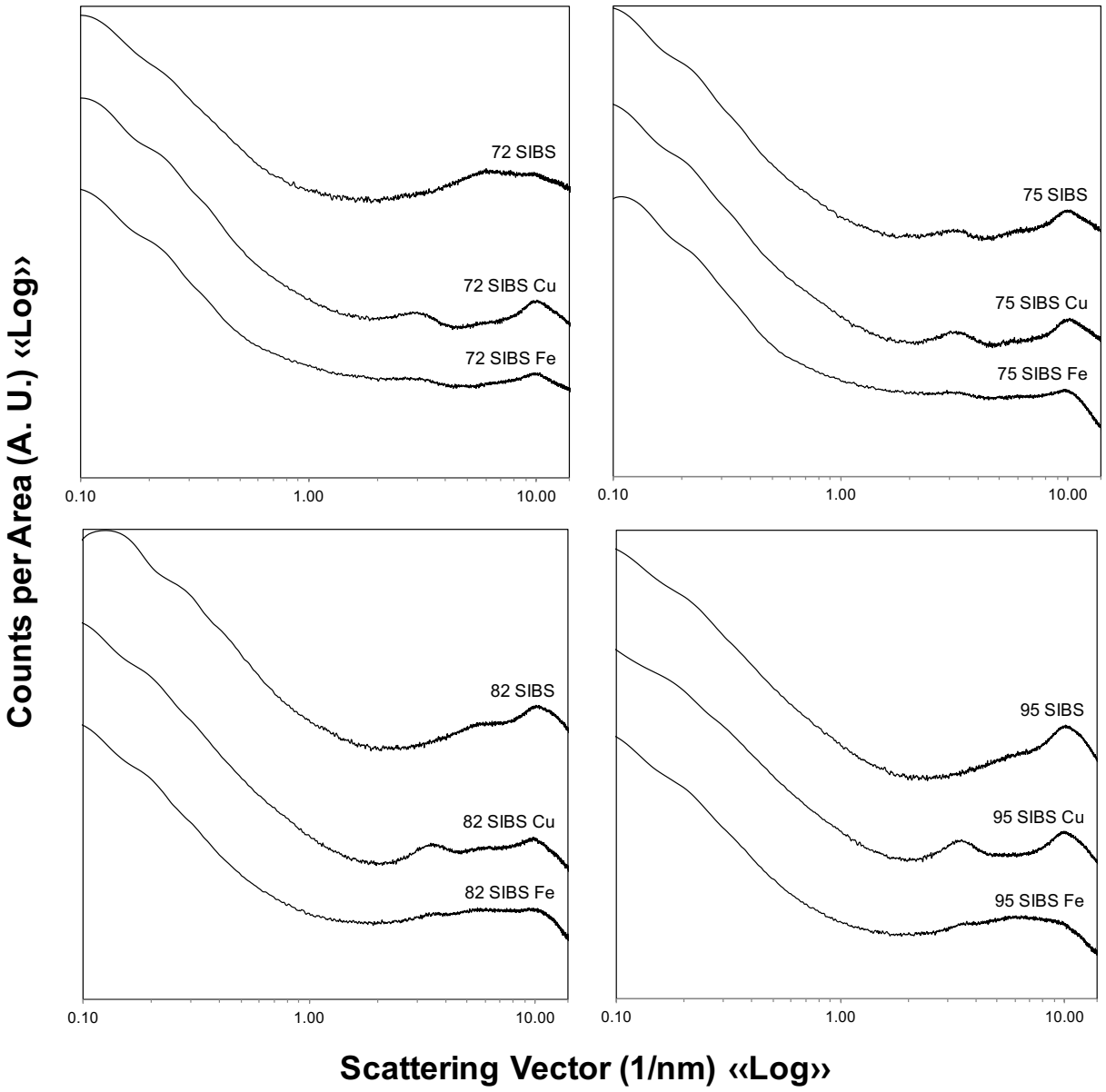

Figure 12. SAXS profiles for copper-exchanged and iron-exchanged sulfonated SIBS.

Table 8. Interstitial distance for copper-exchanged sulfonated SIBS.

Sample	Interstitial Distance 1 (nm)	Interstitial Distance 2 (nm)
72 SIBS Cu	2.04	0.62
75 SIBS Cu	2.01	0.61
82 SIBS Cu	1.80	0.62
95 SIBS Cu	1.78	0.61

In addition to the SAXS, AFM analysis was performed to complement the description of the microstructure of copper-exchanged and iron-exchanged sulfonated SIBS. The phase images for copper-exchanged and iron-exchanged sulfonated SIBS are presented in Figure 13. In general, regardless of the counter-ion substituted, the surface is characterized by the presence of imperfections. However, different sizes of a lamellar structure are visible, at least in a region of the phase image of iron-exchanged sulfonated SIBS at 75% degree of sulfonation. Even though the same lamellar structure can be account for the copper exchanged SIBS at 75% degree of sulfonation, the degree of aggregation is lower than that of iron-exchanged sulfonated SIBS at the same degree of sulfonation. Accordingly, in spite of the complexity of the morphology of copper-exchanged and iron-exchanged sulfonated SIBS, it can be speculated that the degree of aggregation depends on the strength of interaction between the counter-ion and the sulfonic acid groups, and the degree of sulfonation.[39] Even though it was not possible to identify the lamellar structure in the phase images taken for copper-exchanged and iron-exchanged sulfonated SIBS at 82% and 95% degrees of sulfonation, the same lamellar structure is expected as anticipated from the SAXS analysis.

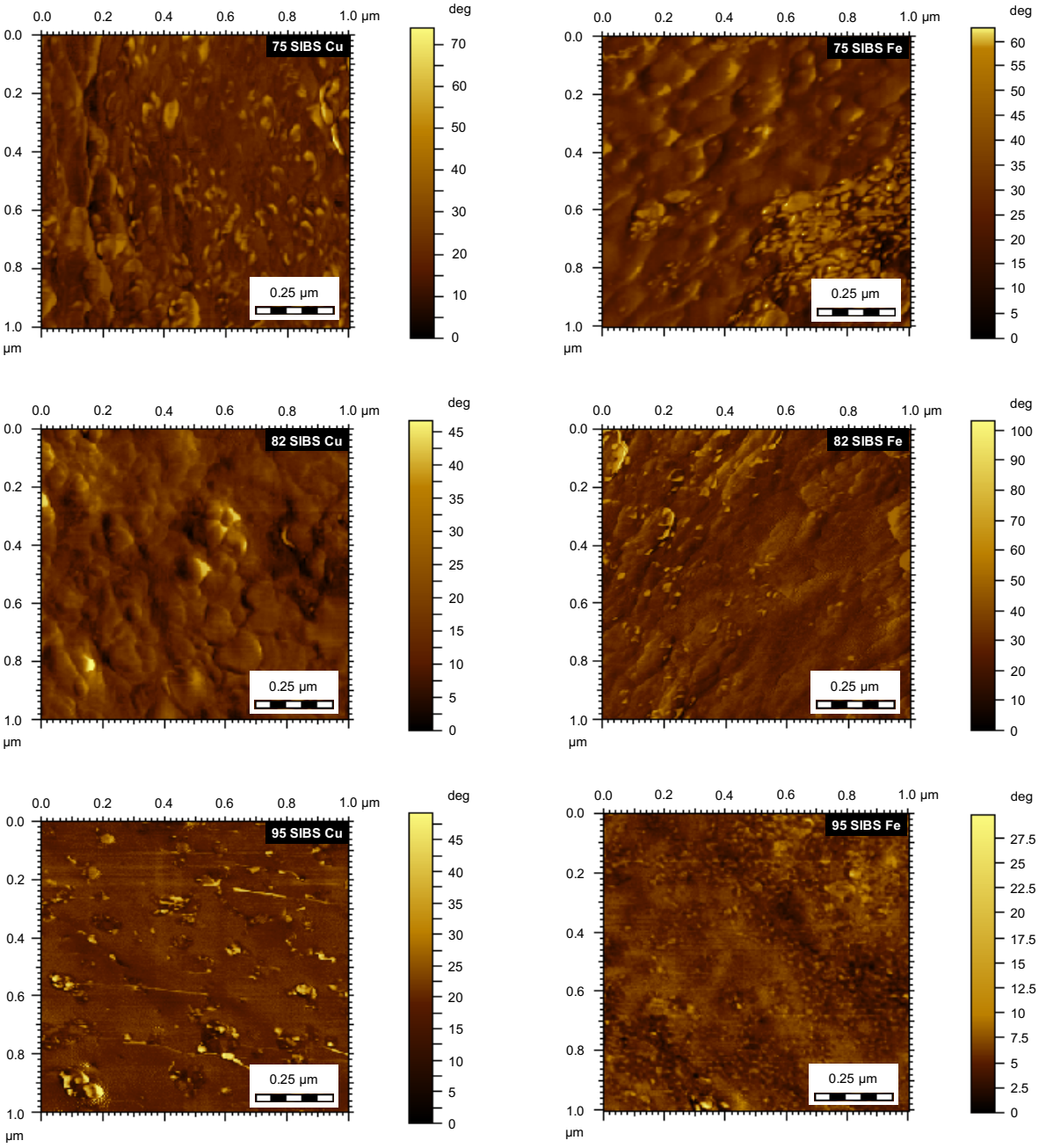

Figure 13. Phase images for copper-exchanged and iron-exchanged sulfonated SIBS.

The surface roughness was determined for copper-exchanged and iron-exchanged sulfonated SIBS and the values are summarized in Table 9. While for each degree of sulfonation the roughness behaves differently, the overall results show that the roughness of copper-exchanged

sulfonated SIBS decreases as the degree of sulfonation increases; and, the roughness of iron-exchanged sulfonated SIBS reaches a maximum value at 82% degrees of sulfonation. It seems that both, the counter-ion and the degree of sulfonation influence in the roughness and imperfections on the surface.[59] Hence, the differences in morphological features, such as surface roughness, may lead to differences in the properties of the copper-exchanged and iron-exchanged sulfonated SIBS properties, such as the water absorption capacity.[39,47]

Table 9. Roughness for copper-exchanged and iron-exchanged sulfonated SIBS.

Sample	Roughness (nm)
75 SIBS Cu	17.54
75 SIBS Fe	9.61
82 SIBS Cu	6.94
82 SIBS Fe	10.82
95 SIBS Cu	3.41
95 SIBS Fe	3.56

Counter-ions may affect the morphology of sulfonated SIBS through a restricted cross-linking and a decrease of charge density on the sulfonic acid groups.[39] Both factors, the restricted cross-linking and the decrease of charge density, influence the water absorption capacity of copper-exchanged and iron-exchanged sulfonated SIBS by increasing the hydrophobicity so not be as swollen as the sulfonated polymer.[39] Since the self-exchange rate of hydration of water molecules depends on the counter-ion and Cu^{2+} has a higher self-exchange rate of water than Fe^{3+}, iron-exchanged sulfonated SIBS shows the lowest water absorption capacity, as seen in Figure 14.[24]

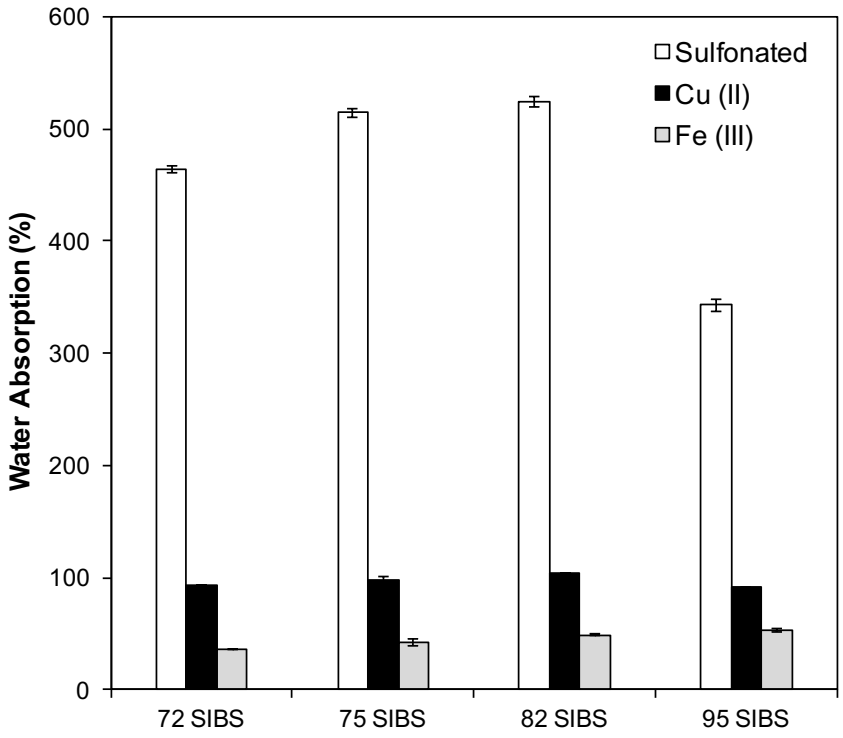

Figure 14. Water absorption capacity of copper-exchanged and iron-exchanged sulfonated SIBS.

Overall, both counter-ions, which are of utmost importance in antibacterial applications, influenced by the morphology and properties of sulfonated SIBS. From a materials characterization standpoint, sulfonated SIBS represented a challenge because the differences imposed by the counter-ions exchanged, required to carry out chemical, thermal and structural analysis to elucidate characteristic features leading to a better understanding of the material in its antibacterial performance.

3.2. Antibacterial performance

3.2.1. *Effect of dilution water*

The rationale for the use of dilution water in the evaluation of the antibacterial activity of sulfonated SIBS against pathogenic bacteria is to prevent population changes in stored bacterial suspensions during the time period of analysis.[11,60] It is particularly useful to select an appropriate buffered solution to ensure that the bacterial species under study are still viable during the course of the antimicrobial assessment.[11] For the antibacterial evaluation of sulfonated SIBS against pathogenic bacteria, a commercial phosphate buffered dilution water recommended for use in the examination of water samples was selected.[61]

The antibacterial activity of sulfonated SIBS was analyzed in batch conditions by adding 100 mL of bacterial suspensions of isolated cultures of *E. coli* and *Enterococci* obtained a natural source, 'Quebrada de Oro', located in Mayagüez, P. R. and which has been reported to be fecally contaminated.[62] This creek was randomly monitored, usually during the morning, and it was found that the average temperature was around 22 ºC, the pH obtained was 8.1 and the average BOD was 7.71. The isolated cultures of each pathogenic bacteria were diluted in the commercial phosphate buffered dilution water. Both bacterial suspensions of *E. coli* and *Enterococci* contained the same initial concentration of 10^1 CFU/100 mL and the membranes were exposed to these pathogenic bacterial suspensions for 10 min. The number of viable cells was determined, and the results are shown in Figure 15.

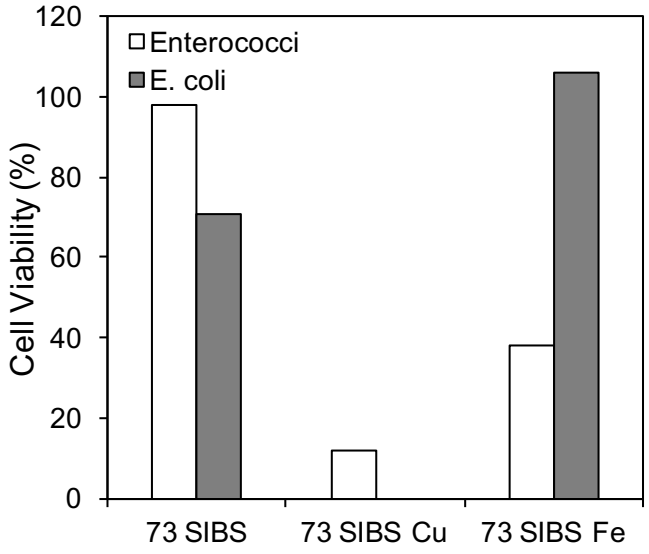

Figure 15. Cell viability results for the evaluation of the antibacterial activity of copper-exchanged and iron-exchanged sulfonated SIBS against *E. coli* and *Enterococci* bacteria.

As seen in Figure 15, for most of the cases, the cell viability decreased with the exposition of the membranes, being copper-exchanged sulfonated SIBS, the membrane showing the lowest cell viability results for *E. coli* and *Enterococci*. Overall, it was expected that after this antibacterial evaluation, we could continue to use over all of these membranes exposed and overcome the cell viability results obtained. However, it was advisable that the membranes used in this experiment be discarded and not used for further antibacterial evaluations because when the exposition was completed, and the membranes were removed from the bacterial suspensions, unexpected superficial changes of the membranes exposed were observed. In addition to the observable changes in the membranes, the formation of turbidity was observed for the bacterial suspensions used in the antibacterial evaluation of the copper-exchanged sulfonated SIBS membranes against *E. coli* and *Enterococci*.

One concern regarding the use of the commercial phosphate buffer is the possibility of compromising the antibacterial performance of sulfonated SIBS when a membrane is exposed to diluted bacterial suspensions. Although the use of a phosphate buffered dilution water serves the purpose of stimulating favorable conditions to maintain cell stability in the pathogenic bacterial suspensions, it may cause restrictions in the performance of sulfonated SIBS.[63] Therefore, by using a similar approach and encouraged by the difficulties encountered, the commercial phosphate buffer was replaced with a phosphate buffered dilution water prepared in the laboratory as described in the method for the detection and enumeration of pathogenic bacteria in water recommended by the Environmental Protection Agency (EPA).[35,36] In addition to monopotassium phosphate, which is the main component of the commercial phosphate buffered dilution water, the phosphate buffered dilution water prepared in the laboratory contained magnesium chloride. The phosphate buffered dilution water prepared in the laboratory improved the chemical nature of the diluent and its influence in the polymer was found to be reliable for the antibacterial evaluation against pathogenic bacteria as suggested by FTIR analysis. FTIR transmittance spectra for sulfonated SIBS, copper-exchanged and iron-exchanged sulfonated SIBS are presented in Figure 16, after each membrane was exposed to deionized water, the phosphate buffered dilution water prepared in the laboratory and the commercial phosphate buffered dilution water. In Figure 16, one should distinguish that for the membrane exposed to the phosphate buffered dilution water prepared in the laboratory, the characteristic bands of the sulfonated polymer were conserved, while for the membranes exposed to the commercial phosphate buffered dilution water, noticeable changes were observed. The FTIR spectra of sulfonated SIBS exposed to the commercial phosphate buffered dilution water showed similar behaviors to those observed for copper-exchanged and iron-exchanged sulfonated SIBS; recall Figure 10. The asymmetric stretching

vibration of the sulfonate group can be observed, thus suggesting that an interaction between counter-ions in the dilution water and the sulfonic acid groups may be occurring. Similarly, the stretching vibration of the sulfonate anion attached to the aromatic ring in the copper-exchanged and iron-exchanged sulfonated SIBS was partly influenced by the commercial phosphate buffered dilution water. The commercial phosphate buffered dilution water also promoted changes in the iron-exchanged sulfonated SIBS at the symmetric stretching vibration of the sulfonate group and the band evidencing the *mono*-substitution in the *para*-position of the aromatic ring.

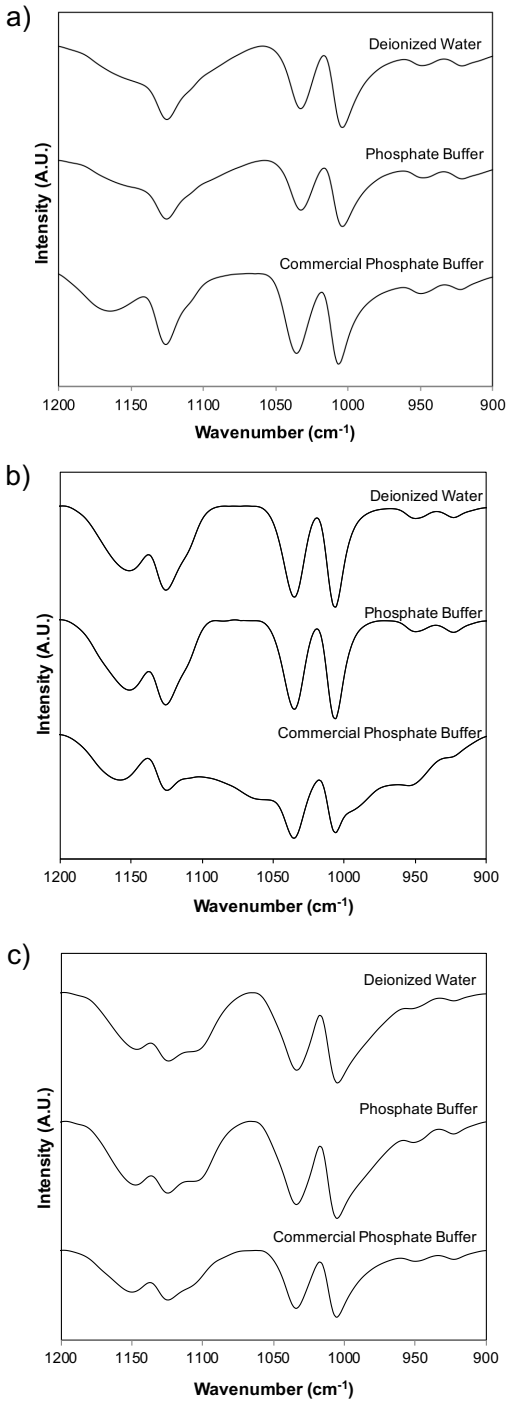

Figure 16. FTIR transmittance spectra of (a) sulfonated SIBS, (b) copper-exchanged sulfonated SIBS and (c) iron-exchanged sulfonated SIBS at 75% degree of sulfonation exposed to deionized water, the phosphate buffered dilution water prepared in the laboratory and the commercial phosphate buffered dilution water.

In addition to the FTIR spectroscopy analysis, the pH of the diluents was evaluated prior and after SIBS membranes were immersed in deionized water, the phosphate buffered dilution water prepared in the laboratory and the commercial phosphate buffered dilution water. The pH measurements are summarized in Table 10. As seen in Table 10, the pH changes when sulfonated SIBS membranes were exposed to a phosphate buffered dilution water. This effect can be attributed to the presence of potassium (K^+) and magnesium (Mg^{+2}) counter-ions in the phosphate buffered dilution water. Although SIBS can resist changes in pH, it has been demonstrated that the incorporation of sulfonic acid groups promotes the counter-ion substitution thus, it is possible that K^+ and Mg^{2+} counter-ions could be neutralizing available ion-exchangeable sites in the membrane.[28,30] Accordingly, it is possible that the presence of K^+ and Mg^{2+} counter-ions is modifying the sulfonated SIBS membrane and its performance in the antibacterial process.[64]

Table 10. pH measurements of the dilution water exposed to copper-exchanged and iron-exchanged sulfonated SIBS membranes.

		pH	
Diluent	**Sample**	initial	final
Deionized water	75 SIBS	6	6
	75 SIBS Cu	6	6
	75 SIBS Fe	6	6
Commercial phosphate buffered dilution water	75 SIBS	8	3
	75 SIBS Cu	8	7
	75 SIBS Fe	8	7
Phosphate buffered dilution water prepared in the laboratory	75 SIBS	6	4
	75 SIBS Cu	6	6
	75 SIBS Fe	6	4

The exact nature of these observations was not determined. However, the conditions under which the antibacterial evaluation took place suggest that there may exist a major issue between the material and the commercial phosphate buffered dilution water; and, that the main cause of the difficulties encountered with the membrane-bacteria interactions could be attributed to a combination of the chemical properties of the commercial phosphate buffered dilution water and the characteristics of the sulfonated SIBS membranes. Hence, in order to account for the necessity of avoiding difficulties with the exposed membrane and maintaining favorable conditions of the pathogenic bacterial suspensions, the phosphate buffered dilution water prepared in the laboratory was selected to bring about appropriate antibacterial evaluations, that is, to achieve a low cell viability without the concern of having to compromise the membrane exposed or the stability of the bacterial suspensions treated.

3.2.2. *Sulfonated SIBS exposed to pathogenic bacteria suspensions*

A control experiment was performed using the MF experimental setup. A membrane of sulfonated SIBS at 72% degree of sulfonation was exposed for 10 min to 100 mL of water samples from a natural source with an initial concentration of 10^2 CFU/100 mL of both *E. coli* and *Enterococci* bacteria. The number of viable cells was determined at 1, 3 and 10 min of treatment and the results are shown in Figure 17. In Figure 17, it can be seen that for both pathogenic bacteria, total inactivation of the population may be difficult to achieve during 10 min of treatment by using a sulfonated SIBS membrane of approximately 50.8 mm of diameter. While the cell viability results for *Enterococci* progressively decreased to nearly 40%, it was observed that the cell viability results for *E. coli* exceeded the 100%. Although both pathogenic bacteria were evaluated simultaneously in 100 mL of water from a natural source, the cell viability results suggest that

Enterococci is more susceptible to sulfonated SIBS membranes than *E. coli*. It is possible that in the water sample analyzed, the probability of interaction of the bacterial cells with all the sulfonic acid groups of the membrane were restricted due to the nature of the source.[59,65] Hence, it is consistent with experimental findings of the analysis of water samples from natural sources, which show that the cell viability of *E. coli* is slightly higher when analyzed in controlled environments.[59]

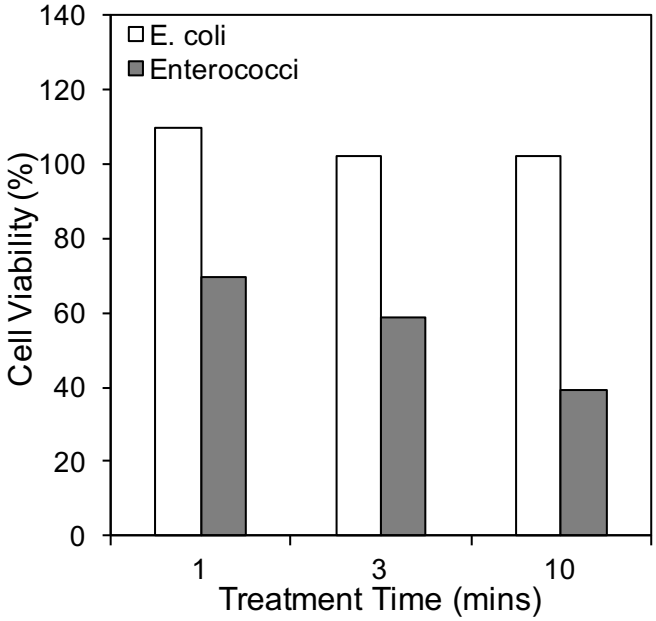

Figure 17. Cell viability results for *E. coli* and *Enterococci* bacteria after sulfonated SIBS membranes were brought into contact with bacteria suspensions.

3.2.3. *Effect of volume*

The antibacterial activity of sulfonated SIBS at 95% degree of sulfonation was evaluated by varying the volume of a water sample from a natural source containing the same initial concentration of 10^4 CFU/100 mL of *E. coli* and *Enterococci* pathogenic bacteria. Sulfonated SIBS and iron-exchanged sulfonated SIBS membranes were analyzed by adding 250 mL (V1) and 100 mL (V2) of water while cooper-exchanged sulfonated SIBS membranes were analyzed by adding 200 mL (V1) and 100 mL (V2) of water from the same source. The number of viable cells was

determined after exposing the membranes of 50.8 mm of diameter for 1 min. The cell viability results for *E. coli* and *Enterococci* are shown in Figure 18 a and b, respectively.

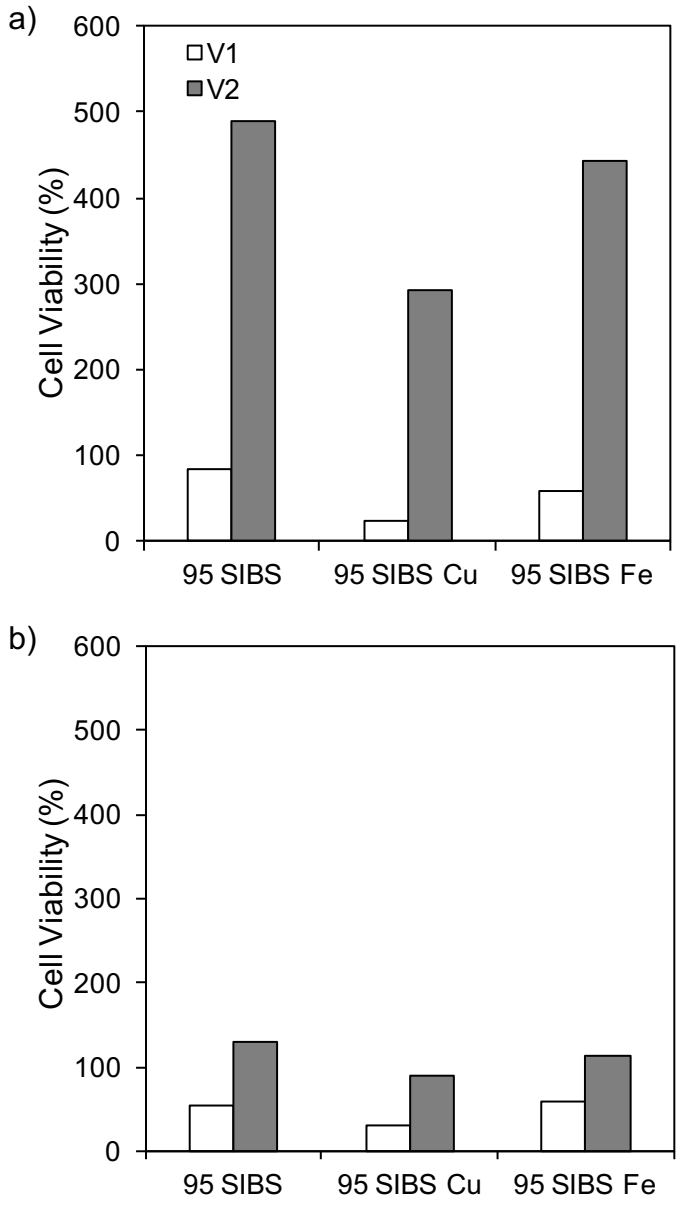

Figure 18. Cell viability results for (a) *Enterococci* and (b) *E. coli* bacteria after sulfonated SIBS membranes were brought into contact with bacteria suspensions of different volume.

According to the cell viability results obtained for both pathogenic bacteria, it can be seen that the water sample volume can dramatically affect the overall antibacterial activity of the sulfonated polymer. The results shown in Figure 18, confirmed that the largest volume analyzed generated the lowest cell viability results for both pathogenic bacteria analyzed while for most of the cases, the lowest volume analyzed, exceeded the 100% of cell viability for *E. coli* and *Enterococci*. The volume effect in the cell viability results could be attributed to the experimental setup. The advantage of using the MF experimental setup for the exposition is not only to encourage an air-tight seal of the membrane but also to promote a pressure gradient through the membrane. This pressure gradient in combination with a larger number of bacteria present in the highest volume may increase the number of bacteria capable of reaching the membrane thus increasing the rate of inactivation.

Regardless of the volume of water analyzed, copper-exchanged sulfonated SIBS successfully inactivated most of both pathogenic bacteria. At the largest volume, iron-exchanged sulfonated SIBS showed lower cell viability results than sulfonated SIBS for *Enterococci*, while for *E. coli* the effect associated with both membranes were almost identical. While at largest volumes the membranes were effective in the inactivation both pathogenic bacteria, copper-exchanged and iron-exchanged sulfonated SIBS membranes yielded better results than the sulfonated SIBS membranes.

3.2.4. *Effect of initial concentration*

The antibacterial activity of copper-exchanged sulfonated SIBS at 95% degree of sulfonation was evaluated by varying the initial concentration of *E. coli* and *Enterococci* pathogenic bacteria. A copper-exchanged sulfonated SIBS membrane, of approximately 50.8 mm

of diameter, was exposed to 20 mL water samples from a natural source for 10 min. Overall, as seen in Figure 19, the lowest initial concentration in the water samples analyzed, 10^2 CFU/100 mL of both pathogenic bacteria, showed the lowest cell viability results for *E. coli* and *Enterococci.* Although *E. coli* and *Enterococci* bacteria were at the same initial concentration, the cell viability results show the inactivation of both bacteria is far better with concentrations in which the cell viability is reduced to a perturbative quantity. Conversely, increasing the initial concentration of both pathogenic bacteria to 10^3 CFU/100 mL had no special advantage in reducing the cell viability. Instead, the increased concentration caused an increase in the overall cell viability.

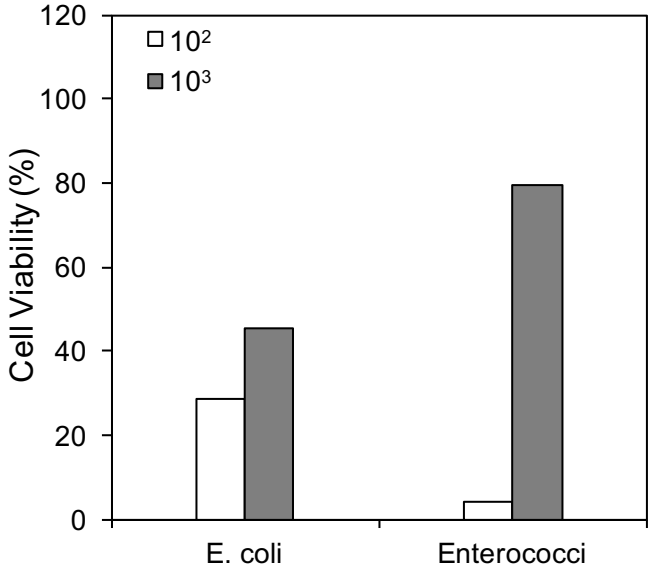

Figure 19. Cell viability results for *E. coli* and *Enterococci* bacteria after copper-exchanged sulfonated SIBS membranes were brought into contact with bacteria suspensions of different initial concentration.

In the range of 10^2 to 10^3 CFU/100 mL, concentration effects could limit the antibacterial activity and in certain cases, increase the cell viability instead of the inactivation of pathogenic bacteria. This suggests that the number of bacteria present in the sample analyzed is high and that the quantity of bacteria, controls the inactivation response. If pathogenic bacteria are available in

a large quantity, the membrane will be much less accessible to a large number of bacteria when compared to a lower concentration. Hence, the lower the concentration, the easier is the cell viability reduced since bacteria interacts with the membrane according to its own accessibility, positively increasing the overall rate of inactivation, as shown in Figure 19. Moreover, based on the results shown in Figure 19, when the concentration is low enough, the copper-exchanged sulfonated SIBS membrane plays a more favorable role in reducing the cell viability of *Enterococci* pathogenic bacteria, even when both pathogenic bacteria are targeted.

3.2.5. *Effect of reusability*

The antibacterial activity of sulfonated SIBS at 72% degree of sulfonation against *E. faecalis* was evaluated with 10 mL of certified bacteria suspension containing an initial concentration of 10^4 CFU/100 mL of *E. faecalis* by using the MF setup. The purpose of this evaluation was to bring about a controlled study of the antibacterial properties of sulfonated SIBS, which would manifest much more clearly for *E. faecalis*, by using the membranes multiple times to describe their reusability. The importance of the reusability is to prove the efficiency of the membrane with a continued usage in the inactivation processes. Cell viability results for *E. faecalis* were determined for 1, 3 and 10 min treatment time, as shown in Figure 20.

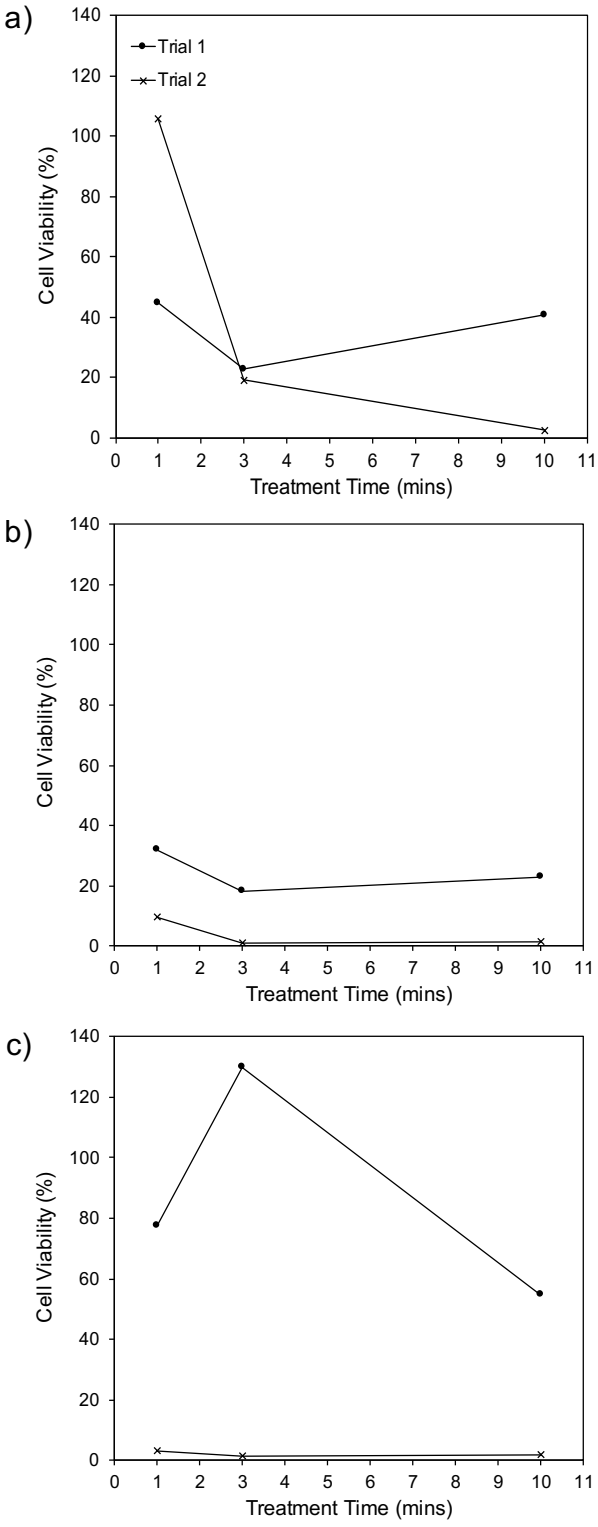

Figure 20. Cell viability results for *E. faecalis* (a) sulfonated SIBS, (b) copper-exchanged sulfonated SIBS, and (c) iron-exchanged sulfonated SIBS membranes at 72% degree of sulfonation were brought into contact with bacteria suspensions multiple times.

The efficiency of sulfonated SIBS is varied, and the cell viability results reached nearly 0% and sometimes exceed the 100%. The ultimate goal is to target a cell viability of 0% at 10 min of treatment and among all membranes tested, second-time reusable membranes reached almost that value. It is possible that, as discussed previously, sulfonated SIBS membranes may be following an exchanged reaction due to the presence of additional groups present in the water analyzed perhaps due to the composition of the dilution water. Hence, the incorporation of additional species could enhance the antibacterial activity of the sulfonated polymer thus increasing the extent of inactivation of the sulfonated polymer reusable membrane.

The cell viability results obtained for *E. faecalis* suggest that the effectiveness of the exposition may vary depending on the treatment time, the counter-ion exchanged and the reusability of the membrane. Overall, at 1 min of treatment, iron-exchanged sulfonated SIBS reusable membrane gives better cell viability results than those observed with copper-exchanged sulfonated SIBS reusable membrane while at 3 min of treatment, both counter-ions behaved similarly thus giving similar cell viability results. Contrary to what was observed for 1 min of treatment, copper-exchanged sulfonated SIBS reusable membrane showed lower cell viability results than iron-exchanged sulfonated SIBS reusable membrane at 10 min of treatment thus suggesting that the lower cell viability results for *E. faecalis* can be accomplished when the bacterial suspensions are continuously exposed for 10 minutes.

3.2.6. *Effect of degree of sulfonation*

The antibacterial activity of sulfonated SIBS was evaluated at two different degrees of sulfonation, 72% and 95%, by using the MF setup. The antibacterial evaluation proceeded using *E. coli* certified bacteria suspensions containing an initial concentration of 10^5 CFU/100 mL. The

cell viability for *E. coli* was determined at 1, 3 and 10 min of treatment, as shown in Figure 21. As seen in Figure 21, for most of the cases, the cell viability results of *E. coli* progressively decrease with increasing the treatment time.

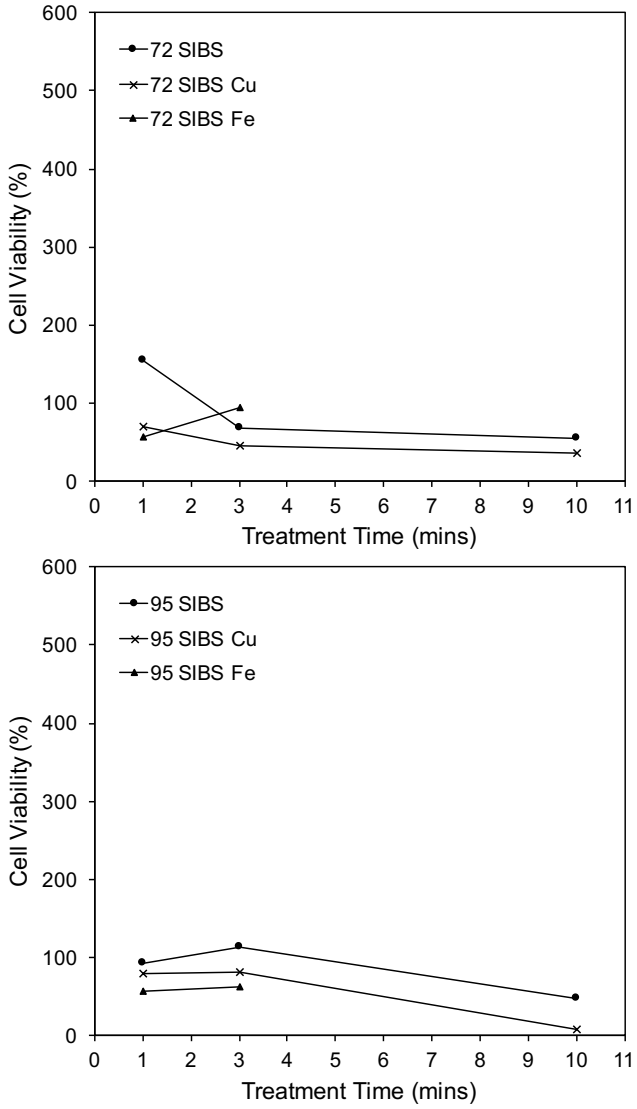

Figure 21. Cell viability results for *E. coli* bacteria after copper-exchanged and iron-exchanged sulfonated SIBS membranes at different degrees of sulfonation were brought into contact with bacteria suspensions.

A deeper insight into the effect of degree of sulfonation and counter-ion exchanged is fundamental to understand the inactivation effectiveness. For instance, at 1 min of treatment, a cell

viability close to 50% can be obtained, regardless of the degree of sulfonation, for iron-exchanged sulfonated SIBS. Contrary to what is observed for sulfonated SIBS at 95% degree of sulfonation at the third minute of treatment, for sulfonated SIBS at 72% degree of sulfonation, with exception of the iron-exchanged sulfonated SIBS membrane, the number of viable cells seems to increase. However, at 3 min of treatment, most of the cell viability results are under 100% but only copper-exchanged sulfonated SIBS at 72% degree of sulfonation provides the lowest result. Overall, the cell viability results presented in Figure 21 suggest that at 10 min of treatment, nearly 0% of cell viability can be obtained for copper-exchanged sulfonated SIBS at 95% degree of sulfonation.

The results obtained suggest that copper-exchanged and iron-exchanged sulfonated SIBS show a particular advantage over sulfonated SIBS. Overall, iron-exchanged sulfonated SIBS exhibit a marked tendency for lowering the cell viability at 1 min of treatment. This effect is being favored at 3 min of treatment but only for 95% degree of sulfonation. On the contrary, it can be observed from Figure 21 that iron-exchanged sulfonated SIBS give rise to cell viability results at 72% degree of sulfonation, being copper-exchanged sulfonated SIBS the membrane at the same degree of sulfonation that gives the lowest cell viability results. Finally, regardless of the degree of sulfonation, copper-exchanged sulfonated SIBS give the best results at 10 min of treatment. Although bacteria suspensions were exposed to iron-exchanged sulfonated SIBS for 10 min, the cell viability results were not successfully obtained at this treatment time.

It should be noted that the cell viability results associated with Cu^{2+} and Fe^{3+} counter-ions did not exceed the 100% when compared to that obtained with the sulfonated polymer at 95% degree of sulfonation. According to the cell viability results obtained at 10 min of treatment, copper-exchanged sulfonated SIBS at 95% degree of sulfonation shows the lowest cell viability results. Mass ratios obtained for copper exchanged sulfonated SIBS, which results were 0.056 g

cation/g SIBS and 0.045 g cation/g SIBS for 95% and 82% degree of sulfonation, respectively, suggest that while the degree of sulfonation is increasing, an increase in the counter-ion quantity can be observed. Although a mass ratio was not obtained for 72% degree of sulfonation, it can be inferred that the inactivation of *E. coli* is dependent on the quantity of the counter-ion exchanged in the SIBS membrane. On the other hand, mass ratios for iron-exchanged sulfonated SIBS were obtained for 95% and 72% degree of sulfonation. The results obtained were 0.038 g cation/g SIBS and 0.036 g cation/g SIBS for 95% and 72% degree of sulfonation, respectively. It should be noted that the rise in the values obtained is minimal thus suggesting that the effect of *E. coli* may be similar even when the degree of sulfonation is increasing. In general, these results suggest that an increase in the quantity of counter-ion as the degree of sulfonation increases, a better *E. coli* inactivation can be achieved.

3.2.7. *Effect of water source*

The use of sulfonated SIBS for the antibacterial evaluations of water from natural sources has its own set of advantages and limitations due to the nature of the source. While the antibacterial activity of sulfonated SIBS is directed to reduce the cell viability of *E. coli* and *Enterococci* pathogenic bacteria, the strength of the interaction may be restricted by the source of the water, mainly for *E. coli*, which has been found to be less susceptible to inactivation in complex environments.[65] Overall, the antibacterial evaluations performed using water from a natural source have shown that copper-exchanged and iron-exchanged sulfonated SIBS can provide substantially low cell viability results for both *E. coli* and *Enterococci*. However, the extent of inactivation of *E. coli* and *Enterococci* varies depending on the water source and the processing conditions. For instance, the cell viability results are lower for certified pathogenic bacteria thus suggesting that

the bacteria interactions with the sulfonated polymer are more frequent in bacterial suspensions prepared in the laboratory than in water from natural sources.

The introduction of selectivity calculations to study the inactivation process represents a way to describe both *E. coli* and *Enterococci* present in a complex environment and their susceptibility to Cu^{2+} and Fe^{3+} counter-ions. The general equation describing the selectivity towards a counter-ion can be written as

$$S_M = \frac{C_i}{C_i + C_j} \quad (7)$$

where S_M represents the selectivity of counter-ion M, C_i represents the death CFU/100 mL of bacteria i and C_i represents the death CFU/100 mL of bacteria j.This relation considers that both pathogenic bacteria were present in water and that the water was treated with either copper-exchanged or iron-exchanged sulfonated SIBS.

The antibacterial activity of sulfonated SIBS against *E. coli* and *Enterococci* was tested in batch conditions by exposing 100 mL of water from a natural source containing 10^3 CFU/100 mL of both pathogenic bacteria to reusable sulfonated SIBS membranes. The number of viable cells was obtained for a 10 min treatment and correspondingly, the selectivity was calculated using equation 7. The selectivity results are summarized in Table 11. As seen in Table 11, the cell viability results for *E. coli* and *Enterococci* using the copper-exchanged sulfonated SIBS are similar. However, copper-exchanged sulfonated SIBS is more selective to *E. coli*. On the other hand, the cell viability results for iron-exchanged sulfonated SIBS are lower for *Enterococci* than for *E. coli*. Therefore, iron-exchanged sulfonated SIBS is more selective to *Enterococci*.

Table 11. Selectivity of copper-exchanged and iron-exchanged sulfonated SIBS to *E. coli* and *Enterococci* bacteria.

	Cell Viability (%)		Selectivity (%)	
Sample	*E. coli*	*Enterococci*	*E. coli*	*Enterococci*
72 SIBS	95	33	6.9	93.1
72 SIBS Cu	73	77	54.1	45.9
72 SIBS Fe	93	58	15.1	84.9

Although the selectivity towards *Enterococci* seems to be great, the total inactivation still remains a challenge. The susceptibility quality of *E. coli* and *Enterococci* suggests that inactivation of these bacteria is independent upon the water source but selective to Cu^{2+} and Fe^{3+} counter-ions, respectively; and, that the antibacterial activity of SIBS suffer from the fact that in most of the cases, it increases the cell viability instead of reducing this value.[16,65]

3.2.8. *SIBS chemical and structure properties after exposure to bacteria suspensions*

It has been found that bacteria tend to adhere to the surface of SIBS promoting the formation of a biofilm.[26] Generally, bacterial adhesion and biofilm formation may stem from a surface charge, hydrophobicity, surface roughness, among other factors.[16,17] However, with the incorporation of sulfonic acid groups into SIBS, the hydrophobicity and surface roughness can be strongly reduced.[28,66] Therefore, it can be speculated that adhesion of bacteria seems uncommonly for sulfonated SIBS.

When the antibacterial evaluation was completed, the membranes were examined by performing a streaking study on the surface of the membranes to verify if the bacteria remained attached to the membrane after the antibacterial evaluation was performed. After 24 h of incubation, fortunately, no evidence for bacterial growth was observed. Most importantly, this study suggested that the adhesion of bacteria to the sulfonated SIBS is not promoted after its exposure to bacteria suspensions.[17,67]

Additionally, following the antibacterial evaluation of sulfonated SIBS against *E. coli*, the membranes were examined to provide an insight into the possible effects caused by the exposure to bacteria suspensions. FTIR, SAXS and AFM analysis were performed to build an understanding based on the fundamental characteristics of the sulfonated polymer, which contributed to the inactivation of pathogenic bacteria.

As shown in Figure 22, FTIR analysis was performed to compare stretching vibrational bands with those of sulfonated SIBS prior exposition to certified bacteria suspensions of *E. coli*. The asymmetric stretching vibration of the sulfonate group of both copper-exchanged and iron-exchanged sulfonated SIBS show a slight shift towards lower wavenumbers, possibly as a consequence due to an interaction with components of the *E. coli* wall membrane after the antibacterial evaluation was performed.

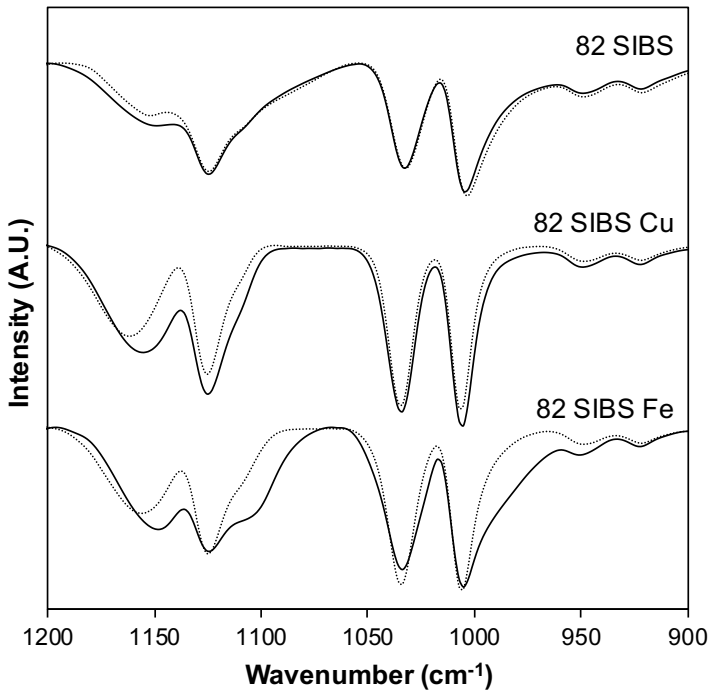

Figure 22. FTIR transmittance spectra for copper-exchanged and iron-exchanged sulfonated SIBS after exposure to *E. coli* bacteria suspensions. The dotted line represents the spectra taken prior exposure to bacteria suspensions while the solid line represents the spectra of the membranes after treatment.

SAXS analysis was performed after the antibacterial evaluation. Scattering profiles are presented in Figure 23. The results associated with the slope of the double-logarithmic plot does not change after the antibacterial evaluation since the same lamellar self-assembled structure with rough interfaces classification of the ionic domains was obtained for the membranes evaluated after the exposition to certified bacteria suspensions of *E. coli*.

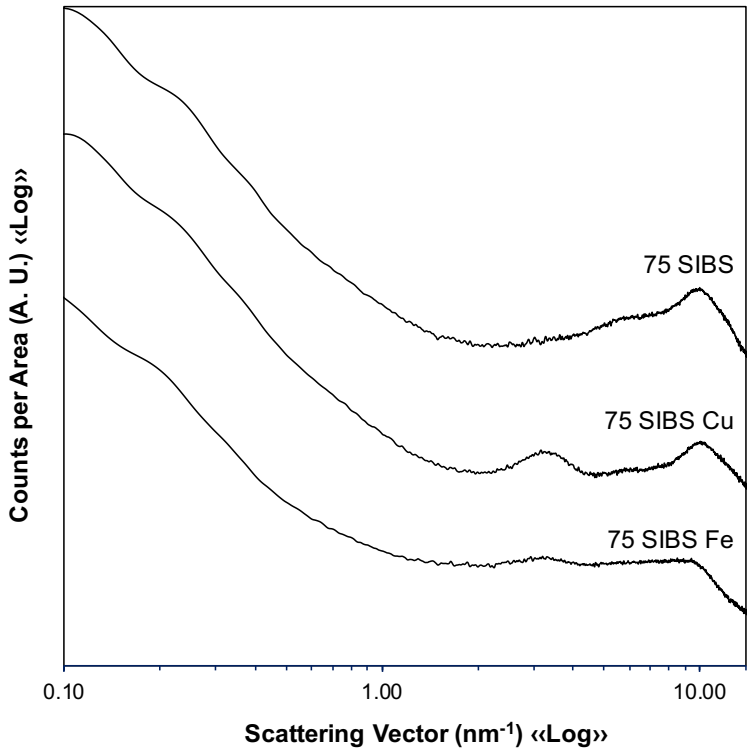

Figure 23. SAXS profiles for copper-exchanged and iron-exchanged sulfonated SIBS after exposure to *E. coli* bacteria suspensions.

In addition to SAXS, AFM phase images were obtained. The phase images of the membranes after the antibacterial evaluation was performed are shown in Figure 24. Although the same scanned area was not studied, in comparison with the AFM phase images obtained for the membranes prior exposition, many differences emerged after the antibacterial evaluation, as seen in Figure 24. Additionally, the surface roughness was obtained, and the results are summarized in Table 12. Many morphological distinctions are well identified and an interesting increase in the surface roughness has emerged for the sulfonated SIBS membrane after the antibacterial evaluation was completed. In the other hand, for copper-exchanged and iron-exchanged sulfonated SIBS, the surface roughness obtained slightly decreased when compared to the values obtained for

the membranes prior exposition; recall Table 4 and Table 9 for surface roughness results of sulfonated SIBS and copper-exchanged and iron-exchanged sulfonated SIBS, respectively.

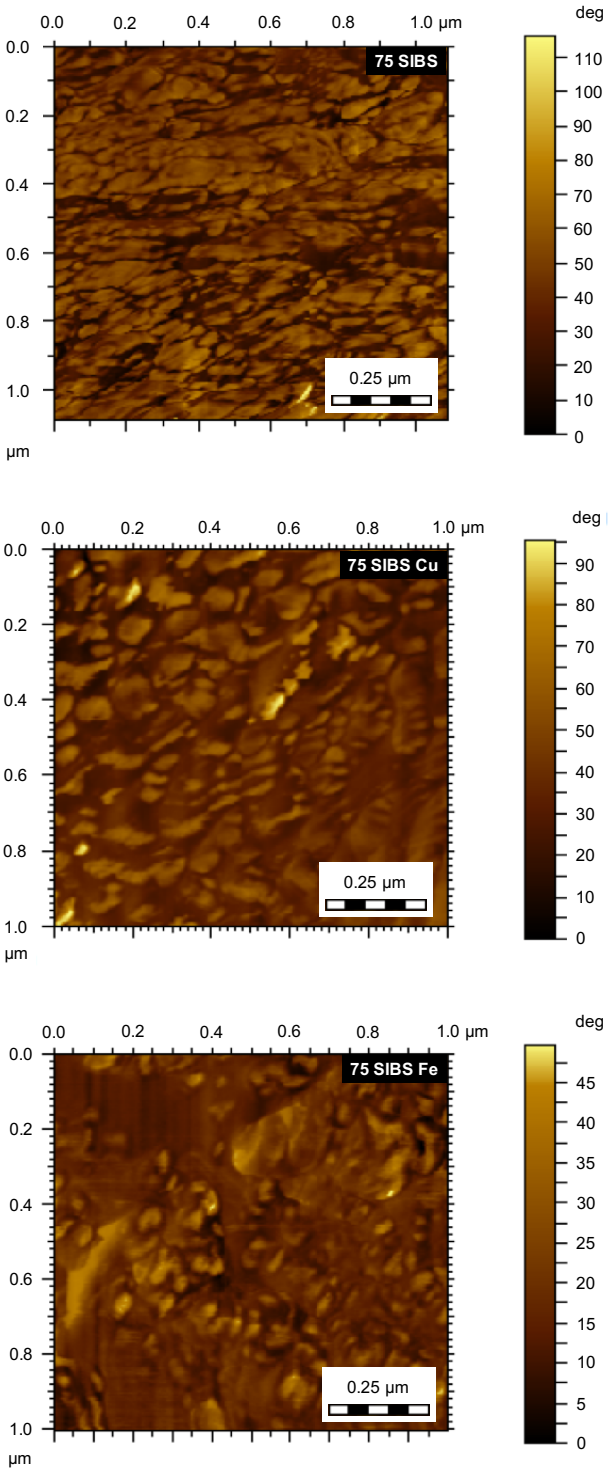

Figure 24. Phase images for copper-exchanged and iron-exchanged sulfonated SIBS after exposure to *E. coli* bacteria suspensions.

Table 12. Roughness for copper-exchanged and iron-exchanged sulfonated SIBS after exposure to *E. coli* bacteria suspensions.

Sample	Roughness (nm)
75 SIBS	13.26
75 SIBS Cu	15.01
75 SIBS Fe	8.28

Overall, although the interactions with the bacteria influenced the physico-chemical properties of the sulfonated SIBS membranes, these can still be used for the inactivation of pathogenic bacteria. As shown for the reusability test, the antibacterial activity of sulfonated SIBS membranes is not entirely compromised after being exposed to bacterial suspensions.

3.2.9. *Basis of pathogenic bacteria inactivation*

While the development of antibacterial polymers has had an important impact on the inactivation processes of pathogenic bacteria, the focus has mainly been on the incorporation of metal-nanoparticles as antibacterial agents in polymeric materials to fulfill the approach of killing bacteria upon contact or by the release of ions from its surface.[16,17,19,20] Although a mechanism of bacterial inactivation has remained unclear, these materials show favorable physico-chemical characteristics for the inactivation of pathogenic bacteria.[13,14,16,17,20,22] Recently, studies have reported the benefits of selecting copper-polymer nanocomposites for antibacterial applications.[16,17,20,22] Copper surfaces which have antibacterial properties can kill bacteria shortly after being in contact, by the release of copper ions from the surface or a combination of both.[17,20,68] With the introduction of copper-polymer nanocomposites, inactivation effects can be observed for Gram-positive and Gram-negative bacteria. However, it was found that these are not equally

susceptible to the antibacterial activity of copper-polymer nanocomposites and that a certain mechanism for the inactivation has not been successfully described.[16]

In general, the cell wall of Gram-positive bacteria has a negative charge due to the presence of major chemical components, such as proteins and teichoic acids.[9,16] Similarly, the outer membrane of Gram-negative bacteria has a negative charge due to the presence of phospholipids.[9,14,15] As for copper surfaces, it appears that the antibacterial activity of copper is attributed to the electron transfer between the negatively charged surface of the bacteria and the positively charged copper ions.[17,22,23,69] Hence, it has been suggested that bacteria inactivation upon contact proceeds by interactions resulting in the damage of the bacteria cell wall or outer membrane and that further damages to the bacteria could happen if released copper ions are capable of reaching the disrupted cell wall or outer membrane and therefore penetrate the bacteria.[16,20,70,71] Although the disruption of the cell wall or outer membrane that ensues can ultimately lead to the inactivation of the bacteria, a detailed description of the initial damage mechanism of the bacteria remains unknown.[70]

Metal-polymer nanocomposites based on silver have been vastly studied for antibacterial applications.[14,17,19,72] Silver-based nanocomposites are typically used against both Gram-positive and Gram-negative bacteria since they exhibit favorable characteristics for the inactivation of both bacteria when used as coatings, through the release of silver ions and other means.[22,68] Although silver has been successfully employed in the inactivation of pathogenic bacteria, using copper is proven to be more cost-effective.[17] Among metal-polymer nanocomposites, iron-based nanocomposites have been evaluated, showing similar approaches for contact-killing, the release of ions or the combination of both.[20,68]

According to the characterization results, it appears that sulfonated SIBS membranes are not losing their counter-ions. Hence, it can be speculated that the bacterial inactivation approach of sulfonated SIBS is associated to the inactivation of pathogenic bacteria upon contact and not through the release of counter-ions. Although the physico-chemical properties of sulfonated SIBS have been influenced by interactions with pathogenic bacteria, it has been observed that these changes do not compromise the antibacterial properties of the membrane. Therefore, it can be suggested that the inactivation of pathogenic bacteria may be caused mainly by structural damages on the bacteria cell wall or outer membrane promoted by the interactions with the Cu^{2+} and Fe^{3+} counter-ions exchanged in the sulfonated polymer, in a similar sense of a copper surface.[13,71]

4 Conclusions and recommendations

The antibacterial evaluation of copper-exchanged and iron-exchanged sulfonated SIBS was carried out by assaying the presence of *E. coli* and *Enterococci* bacteria after the membranes were brought into contact with bacteria suspensions. Based on antibacterial studies performed, the cell viability results obtained for both *E. coli* and *Enterococci* bacteria, provided information about the efficiency of SIBS membrane on the inactivation of both pathogenic bacteria, necessary to adequately develop treatment strategies demanding safe drinking water. In accordance with the uniformity in the methodology of quantifying the cell viability results, the time period of analysis, the degree of sulfonation and the counter-ions exchanged in the SIBS membrane, and some other important factors were taken into consideration when describing the effects and the efficiency of the inactivation of pathogenic bacteria.

While making the appropriate choice of experimental conditions and the metal-polymer nanocomposites with optimal antibacterial properties, it should be stressed that because of the presence of Cu^{2+} and Fe^{3+} counter-ions in the sulfonated SIBS membranes, nearly 0% cell viability

results were obtained after the exposure of copper-exchanged and iron-exchanged sulfonated SIBS to pathogenic bacteria suspensions. Concerning the antibacterial activity of copper-exchanged and iron-exchanged sulfonated SIBS membranes, for their inactivation potential to be efficiently harnessed, understanding the mechanism of bacteria inactivation is instrumental. To identify the steps in the inactivation process opens up the possibility to describe more effectively key interactions to develop more efficient antibacterial strategies for the use of metal-polymer nanocomposites in antibacterial applications. However, pathogenic bacteria have complicated properties and their surface components involve simultaneous interactions of multiple components. Nevertheless, a detailed study employing AFM could be performed to measure the adhesive forces in the membrane, which may lead to a better understanding of the interactions between the bacteria and the metal-polymer nanocomposite. By functionalizing the tip of the AFM with certain bacteria, preferably *E. coli* and *E. faecalis*, it could be possible to determine whether bacteria are attracted or repelled by the polymer surface. Also, AFM could be used to characterize the surface of each bacteria to further study specific interactions with the metal-polymer nanocomposite membrane. Most importantly, it could help in the contribution of describing the effect of possible events in the interaction mechanism, which may lead to the identification of significant steps involved in the kinetics of the inactivation process.

Overall, the results of the antibacterial evaluations performed suggested that *Enterococci* is more susceptible to inactivation than *E. coli* and that copper-exchanged sulfonated SIBS successfully inactivated most of both pathogenic bacteria. Nevertheless, it was found that copper-exchanged sulfonated SIBS is more selective to *E. coli* and iron-exchanged sulfonated SIBS is more selective to *Enterococci* bacteria. According to the cell viability results obtained, the extent of inactivation varies depending on the water source and the processing conditions. The cell

viability results are lower for certified pathogenic bacteria suspensions than for water from natural sources. The use of certified bacterial suspensions implies exclusion of potential interactions between additional species contained in water from natural sources. Water from natural sources contained a varied composition and can dramatically difficult the action of the sulfonated polymer against targeted pathogenic bacteria. However, although the extent of inactivation pathogenic bacteria varies depending on the water source and each antibacterial evaluation was performed at different conditions, it was observed that the inactivation process is strongly influenced by the degree of sulfonation, in some cases, and counter-ions exchanged in the sulfonated polymer. For instance, increasing the degree of sulfonation increases the Cu^{2+} quantity in the membrane thus leading to the inactivation of *E. coli*. While the inactivation of *E. coli* is dependent on the quantity of the counter-ion exchanged in the SIBS membrane, the cell viability of *E. coli* progressively decreases with increasing the treatment time in most of the cases.

The importance of developing environmentally safe materials capable of inactivating harmful microorganisms are also expected to maintain its antibacterial properties while providing source protection. Although it has been suggested that a biofilm formation is not promoted for sulfonated SIBS, a fouling test could be performed to confirm if the continuous usage of the membrane contributes to a decrease in the effectiveness of the antibacterial properties of the membrane or does not affect its antibacterial properties. The physico-chemical properties of copper-exchanged and iron-exchanged sulfonated SIBS were influenced by the exposure to bacteria suspensions. However, the antibacterial properties of the membranes were not compromised since, with reusable membranes, nearly 0% cell viability results were achieved.

References

(1) WHO. *Guidelines for drinking-water quality : first addendum to the third edition, volume 1 : reccommendations*; Geneva: WHO, 2006.

(2) Hrudey, S. E.; Hrudey, E. J. *Water Intell. Online* **2015**, *5*.

(3) WHO/UNICEF. *WHO Libr.* **2010**, 60.

(4) UNICEF and WHO. *Drinking water*; 2012.

(5) WHO/UNICEF. **2015**.

(6) USEPA. *United States Environ. Prot. Agency,Office Water Regul. Stand. Criteria Stand. Div.* **1986**, No. January, EPA440/5-84-002.

(7) USEPA. *U. S. Environ. Prot. Agency* **2012**, 1–69.

(8) Cabral, J. P. S. *International Journal of Environmental Research and Public Health*. October 2010, pp 3657–3703.

(9) Rohilla, A. *Handbook of bacteriology*; Oxford Book Co.: Jaipur, 2010.

(10) Hazen, T. C. *Toxic. Assess.* **1988**, *3* (5), 461–477.

(11) Liao, C. H.; Shollenberger, L. M. *Lett. Appl. Microbiol.* **2003**, *37* (1), 45–50.

(12) Mañas, P.; Pagán, R. In *Journal of Applied Microbiology*; 2005; Vol. 98, pp 1387–1399.

(13) Cho, M.; Kim, J.; Kim, J. Y.; Yoon, J.; Kim, J. H. *Water Res.* **2010**, *44* (11), 3410–3418.

(14) Siedenbiedel, F.; Tiller, J. C. *Polymers*. January 2012, pp 46–71.

(15) Catania, C.; Thomas, A. W.; Bazan, G. C. *Chem. Sci.* **2016**, *7* (3), 2023–2029.

(16) Tamayo, L.; Azócar, M.; Kogan, M.; Riveros, A.; Páez, M. *Mater. Sci. Eng. C* **2016**, *69*, 1391–1409.

(17) Armentano, I.; Arciola, C. R.; Fortunati, E.; Ferrari, D.; Mattioli, S.; Amoroso, C. F.; Rizzo,

J.; Kenny, J. M.; Imbriani, M.; Visai, L. *Scientific World Journal*. 2014, pp 1–18.

(18) Madkour, A. E.; Dabkowski, J. M.; Nüsslein, K.; Tew, G. N. *Langmuir* **2009**, *25* (2), 1060–1067.

(19) Muñoz-Bonilla, A.; Fernández-García, M. *Prog. Polym. Sci.* **2012**, *37* (2), 281–339.

(20) Mathews, S.; Hans, M.; Mücklich, F.; Solioz, M. *Appl. Environ. Microbiol.* **2013**, *79* (8), 2605–2611.

(21) Álvarez-Paino, M.; Muñoz-Bonilla, A.; Fernández-García, M. *Nanomaterials* **2017**, *7* (3), 48.

(22) Vimbela, G.; Ngo, S. M.; Fraze, C.; Yang, L.; Stout, D. A. *Int. J. Nanomedicine* **2017**, *Volume 12*, 3941–3965.

(23) Akhavan, O.; Ghaderi, E. *Surf. Coatings Technol.* **2010**, *205* (1), 219–223.

(24) Okada, T.; Ayato, Y.; Yuasa, M.; Sekine, I. *J. Phys. Chem. B* **1999**, *103* (17), 3315–3322.

(25) Yuan, S.; Li, Y.; Luan, S.; Shi, H.; Yan, S.; Yin, J.; Luan, S. F.; Zhao, J.; Yang, H. W.; Shi, H. C.; Jin, J.; Li, X. M.; Liu, J. C.; Wang, J. W.; Yin, J. H.; Stagnaro, P.; Puskas, J. E.; Foreman-Orlowski, E. A.; Lim, G. T.; Porosky, S. E.; Evancho-Chapman, M. M.; Schmidt, S. P.; Fray, M. El; Piatek, M.; Prowans, P.; Lovejoy, K.; Yang, H. W.; Luan, S. F.; Zhao, J.; Shi, H. C.; Li, X. M.; Song, L. J.; Jin, J.; Shi, Q.; Yin, J. H.; Shi, D.; Stagnaro, P.; Puskas, J. E.; Chen, Y. H.; Lim, G. T.; Puskas, J. E.; Reneker, D. H.; Jakli, A.; Horton, W. E.; Pinchuk, L.; Wilson, G. J.; Barry, J. J.; Schoephoerster, R. T.; Parel, J. M.; Kennedy, J. P.; Fray, M. El; Prowans, P.; Puskas, J. E.; Altstädt, V.; Hook, A. L.; Chang, C. Y.; Yang, J.; Luckett, J.; Cockayne, A.; Atkinson, S.; Mei, Y.; Bayston, R.; Irvine, D. J.; Langer, R.; Anderson, D. G.; Williams, P.; Davies, M. C.; Alexander, M. R.; Yuan, S.; Zhao, J.; Luan, S.; Yan, S.; Zheng, W.; Yin, J.; Yuan, S. S.; Li, Z. H.; Zhao, J.; Luan, S. F.; Ma, J.; Song,

L. J.; Shi, H. C.; Jin, J.; Yin, J. H.; Yuan, S.; Luan, S.; Yan, S.; Shi, H.; Yin, J.; Hadjesfandiari, N.; Yu, K.; Mei, Y.; Kizhakkedathu, J. N.; Aumsuwan, N.; McConnell, M. S.; Urban, M. W.; Luo, J.; Porteous, N.; Lin, J.; Sun, Y.; Ding, X.; Yang, C.; Lim, T. P.; Hsu, L. Y.; Engler, A. C.; Hedrick, J. L.; Yang, Y. Y.; Perelshtein, I.; Ruderman, E.; Perkas, N.; Tzanov, T.; Beddow, J.; Joyce, E.; Mason, T. J.; Blanes, M.; Molla, K.; Patlolla, A.; Frenkel, A. I.; Gedanken, A.; Jiang, F. G.; Yeh, C. K.; Wen, J. C.; Sun, Y. Y.; Petkova, P.; Francesko, A.; Fernandes, M. M.; Mendoza, E.; Perelshtein, I.; Gedanken, A.; Tzanov, T.; Cao, Z. B.; Sun, X. B.; Yao, J. R.; Sun, Y. Y.; Zille, A.; Fernandes, M. M.; Francesko, A.; Tzanov, T.; Fernandes, M.; Oliveira, F. R.; Almeida, L.; Amorim, T.; Carneiro, N.; Esteves, M. F.; Souto, A. P.; Mi, L.; Jiang, S. Y.; Xu, F. J.; Liu, L. Y.; Yang, W. T.; Kang, E. T.; Neoh, K. G.; Ma, H. W.; Hyun, J. H.; Stiller, P.; Chilkoti, A.; Cheng, G.; Xite, H.; Zhang, Z.; Chen, S. F.; Jiang, S. Y.; Cao, Z.; Mi, L.; Mendiola, J.; Ella-Menye, J. R.; Zhang, L.; Xue, H.; Jiang, S.; Zhao, J.; Song, L. J.; Shi, Q.; Luan, S. F.; Yin, J. H.; Lin, W. F.; Ma, G. L.; Ji, F. Q.; Zhang, J.; Wang, L. G.; Sun, H. T.; Chen, S. F.; Yin, H. Y.; Akasaki, T.; Sun, T. L.; Nakajima, T.; Kurokawa, T.; Nonoyama, T.; Taira, T.; Saruwatari, Y.; Gong, J. P.; Jiang, S. Y.; Cao, Z. Q.; Blanco, C. D.; Ortner, A.; Dimitrov, R.; Navarro, A.; Mendoza, E.; Tzanov, T.; Zhao, W. W.; Ye, Q.; Hu, H. Y.; Wang, X. L.; Zhou, F.; Li, M.; Neoh, K. G.; Kang, E. T.; Lau, T.; Chiong, E.; Jiang, J. H.; Zhu, L. P.; Zhu, L. J.; Zhang, H. T.; Zhu, B. K.; Xu, Y. Y.; Alswieleh, A. M.; Cheng, N.; Canton, I.; Ustbas, B.; Xue, X.; Ladmiral, V.; Xia, S. J.; Ducker, R. E.; Zubir, O. El; Cartron, M. L.; Hunter, C. N.; Leggett, G. J.; Armes, S. P.; Ladd, J.; Zhang, Z.; Chen, S.; Hower, J. C.; Jiang, S.; Yu, Q.; Wu, Z. Q.; Chen, H.; Mi, L.; Jiang, S. Y.; Liu, S. Q.; Yang, C.; Huang, Y.; Ding, X.; Li, Y.; Fan, W. M.; Hedrick, J. L.; Yang, Y. Y.; Itsuno, S.; Uchikoshi, K.; Ito, K.; Li, T. L.; Ning, F. L.; Xie, J. W.; Chen,

D. Y.; Jiang, M.; Yang, W. J.; Cai, T.; Neoh, K. G.; Kang, E. T.; Dickinson, G. H.; Teo, S. L. M.; Rittschof, D.; Gunkel, G.; Huck, W. T. S.; Busscher, H. J.; Mei, H. C. van der; Subbiahdoss, G.; Jutte, P. C.; Dungen, J. J. A. M. van den; Zaat, S. A. J.; Schultz, M. J.; Grainger, D. W.; Jiang, H.; Wang, X. B.; Li, C. Y.; Li, J. S.; Xu, F. J.; Mao, C.; Yang, W. T.; Shen, J.; He, Q.; Gong, K.; Ao, Q.; Ma, T.; Yan, Y. F.; Gong, Y. D.; Zhang, X. F.; Goswami, S.; Thiyagarajan, D.; Samanta, S.; Das, G.; Ramesh, A.; Asri, L. A. T. W.; Crismaru, M.; Roest, S.; Chen, Y.; Ivashenko, O.; Rudolf, P.; Tiller, J. C.; Mei, H. C. van der; Loontjens, T. J. A.; Busscher, H. J. *J. Mater. Chem. B* **2016**, *4* (6), 1081–1089.

(26) Yuan, S.; Zhao, J.; Luan, S.; Yan, S.; Zheng, W.; Yin, J. *ACS Appl. Mater. Interfaces* **2014**, *6* (20), 18078–18086.

(27) Elabd, Y. A.; Napadensky, E. *Polymer (Guildf).* **2004**, *45* (9), 3037–3043.

(28) Avilés-Barreto, S. L.; Suleiman, D. *J. Appl. Polym. Sci.* **2013**, *129* (4), 2294–2304.

(29) Yuan, S.; Li, Z.; Song, L.; Shi, H.; Luan, S.; Yin, J. *ACS Appl. Mater. Interfaces* **2016**, *8* (33), 21214–21220.

(30) Pinchuk, L.; Wilson, G. J.; Barry, J. J.; Schoephoerster, R. T.; Parel, J. M.; Kennedy, J. P. *Biomaterials* **2008**, *29* (4), 448–460.

(31) Castagna, A. M.; Wang, W.; Winey, K. I.; Runt, J. *Macromolecules* **2010**, *43* (24), 10498–10504.

(32) Unnikrishnan, L.; Nayak, S. K.; Mohanty, S.; Sarkhel, G. *Polym. - Plast. Technol. Eng.* **2010**, *49* (14), 1419–1427.

(33) Tanak, Y. *Ion exchange membranes: Fundamentals and applications*, 1st ed.; Tanaka, Y., Ed.; Membrane science and technology series; Elsevier: Amsterdam ; Boston, 2007; Vol. 12.

(34) Schnablegger, H.; Singh, Y. *Ant. Paar* **2011**, 1–99.

(35) USEPA. *Sci. Technol.* **2002**, No. September, 14.

(36) USEPA. *Stand. Methods* **2002**, No. September, 18.

(37) Alonso, A.; Muñoz-Berbel, X.; Vigués, N.; MacAnás, J.; Muñoz, M.; Mas, J.; Muraviev, D. N. *Langmuir* **2012**, *28* (1), 783–790.

(38) Kučera, F. Homogeneous and heterogeneous sulfonation of polystyrene, 2001, Vol. 38.

(39) Tant, M. R.; Mauritz, K. A.; Wilkes, G. L. *Ionomers*; Springer Netherlands: Dordrecht, 1997.

(40) Suleiman, D.; Napadensky, E.; Sloan, J. M.; Crawford, D. M. *Thermochim. Acta* **2007**, *460* (1–2), 35–40.

(41) Larkin, P. *Infrared and raman spectroscopy: Principles and spectral interpretation*; Elsevier: Amsterdam ; Boston, 2011.

(42) Elmer, P. Thermogravimetric analysis (TGA): A beginner's guide.

(43) Socrates, G. *Infrared and raman characteristic group frequencies*, 3. ed., re.; Wiley: Chichester, 2004.

(44) Ding, J.; Chuy, C.; Holdcroft, S. *Macromolecules* **2002**, *35* (4), 1348–1355.

(45) Widmann, G. 2001.

(46) Suleiman, D.; Elabd, Y. A.; Napadensky, E.; Sloan, J. M.; Crawford, D. M. *Thermochim. Acta* **2005**, *430* (1–2), 149–154.

(47) *Macromolecular engineering: precise synthesis, materials properties, applications*; Matyjaszewski, K., Gnanou, Y., Leibler, L., Eds.; Wiley-VCH: Weinheim, 2007.

(48) Drobny, J. G. *Handbook of thermoplastic elastomers*, Second Edi.; PDL HANDBOOK SERIES; ELSEVIER: Amsterdam, 2014.

(49) Riviere, J. C.; Myhra, S.; Editors. *Handbook of surface and interface analysis: Methods for problemsolving*, 2nd ed.; Rivière, J. C., Myhra, S., Eds.; CRC Press: Boca Raton, 2009.

(50) Mendil-Jakani, H.; Zamanillo Lopez, I.; Legrand, P. M.; Mareau, V. H.; Gonon, L. *Phys. Chem. Chem. Phys.* **2014**, *16* (23), 11243–11250.

(51) Utracki, L. A. *Multiphase polymers: blends and ionomers*; Utracki, L. A., Weiss, R. A., American Chemical Society, Chemical Institute of Canada, American Chemical Society, Eds.; ACS symposium series; American Chemical Society: Washington, DC, 1989; Vol. 395.

(52) Ortiz-Negrón, A.; Suleiman, D. *J. Appl. Polym. Sci.* **2015**, *132* (41).

(53) Suleiman, D.; Padovani, A. M.; Negrõn, A. A.; Sloan, J. M.; Napadensky, E.; Crawford, D. M. *J. Appl. Polym. Sci.* **2014**, *131* (11), n/a-n/a.

(54) Yu, J.; Magonov, S. N. *Appl. Note, Agil. Technol.* **2007**.

(55) KEYENCE. **2012**.

(56) Martins, C. R.; Ruggeri, G.; De Paoli, M. A. *J. Braz. Chem. Soc.* **2003**, *14* (5), 797–802.

(57) Chen, M.; Ma, J.; Wang, Z.; Zhang, X.; Wu, Z. *RSC Adv.* **2017**, *7* (58), 36555–36561.

(58) Büchi, F. N.; Schmidt, T. J.; Inaba, M. *Polymer electrolyte fuel cell durability*; Büchi, F. N., Inaba, M., Schmidt, T. J., Eds.; Springer New York: New York, NY, 2009.

(59) Preedy, E.; Perni, S.; Nipiĉ, D.; Bohinc, K.; Prokopovich, P. *Langmuir* **2014**, *30* (31), 9466–9476.

(60) Russell, A. D.; Hugo, W. B.; J, A. G. A. *Principles and practive of disinfection preservation & sterilization*, 4. ed.; Russell, A., Hugo, W. B., Ayliffe, G. A. J., Fraise, A. P., Lambert, P. A., Maillard, J.-Y., Eds.; Blackwell Publ: Oxford, 2004.

(61) AMERICAN PUBLIC HEALTH ASSOCIATION (APHA). American Water Works

Association, 2017; Vol. 23.

(62) Junta Calidad Ambiental. 2013, p 305.

(63) Bordner, R.; Winter, J. EPA December 1978, p 338.

(64) Rincón, A. G.; Pulgarin, C. *Appl. Catal. B Environ.* **2004**, *51* (4), 283–302.

(65) Noble, R. T.; Lee, I. M.; Schiff, K. C. *J. Appl. Microbiol.* **2004**, *96* (3), 464–472.

(66) Jagtap, R. N.; Ambre, A. H. *Indian J. Eng. Mater. Sci.* **2006**, *13* (4), 368–384.

(67) An, Y. H.; Friedman, R. J. *Handbook of bacterial adhesion: principles, methods, and applications*; An, Y. H., Friedman, R. J., Eds.; Humana Press: Totowa, N.J, 2010.

(68) Hasan, J.; Crawford, R. J.; Ivanova, E. P. *Trends Biotechnol.* **2013**, *31* (5), 295–304.

(69) Chen, S. F.; Li, J. P.; Qian, K.; Xu, W. P.; Lu, Y.; Huang, W. X.; Yu, S. H. *Nano Res.* **2010**, *3* (4), 244–255.

(70) Tiller, J. C.; Liao, C.-J.; Lewis, K.; Klibanov, A. M. *Proc. Natl. Acad. Sci.* **2001**, *98* (11), 5981–5985.

(71) *Handbook of food safety engineering*, 1. ed.; Sun, D.-W., Ed.; Wiley-Blackwell: Chichester, 2011.

(72) Pal, S.; Tak, Y. K.; Song, J. M. *J. Biol. Chem.* **2015**, *290* (42), 1712–1720.

Appendix

A. Agar composition

Table A.1. Composition of MI Agar

Component	Quantity
Proteose Peptone #3	5.0 g
Yeast Extract	3.0 g
β-D-Lactose	1.0 g
4-Methylumbelliferyl-β-D-Galactopyranoside (MUGal) (Final concentration 100µg/mL)	0.1 g
Indxyl-β-D-Glucuronide (IBDG) (Final concentration 320 µg/mL)	0.32 g
NaCl	7.5 g
K_2HPO_4	3.3 g
KH_2PO_4	1.0 g
Sodium Lauryl Sulfate	0.2 g
Sodium Desoxycholate	0.1 g
Agar	15.0 g
Reagent-Grade Distilled Water	1000 mL

Table A.2. Composition of mEI Agar

Component	Quantity
Peptone	10.0 g
Sodium Chloride	15.0 g
Yeast Extract	30.0 g
Esculin	1.0 g
Actidione (Cycloheximide)	0.05 g
Sodium Azide	0.15 g
Agar	15.0 g
Reagent-Grade Distilled Water	1.0 L